Electroweak Form Factors of Heavy-Light Mesons for Space- and Timelike Momentum Transfer

Oliver Senekowitsch

DIPLOMARBEIT
zur Erlangung des akademischen Grades eines Magisters an der
Naturwissenschaftlichen Fakultät der Karl-Franzens-Universität Graz

Betreuer:
Ao. Univ.-Prof. Mag. Dr. Wolfgang Schweiger
Institut für Physik, FB Theoretische Physik

June 4, 2014

Contents

Chapter 1

Introduction

Since hadrons are known to possess a non-trivial structure – they appear to consist of point-like constituents in deep inelastic electron-proton scattering for example – both, experimentalists and theorists try to decipher this inner structure. The combination of the observed scaling behavior and Gell-Mann's famous hadron classification into SU(3) multiplets led to the idea that baryons and mesons are made up by (at least) either three quarks or a quark and an antiquark, respectively. Within a quantum-field theoretical framework these "valence-degrees-of-freedom" are supplemented by gluons, which mediate the strong force between quarks, and by additional quarks and antiquarks filling the Dirac sea. The simplest possibility to learn about the hadron structure, however, is to describe hadrons within quantum mechanics using a valence- or constituent-quark model. In order to analyze the weak structure of heavy-light mesons, as it is observable in semileptonic transitions, we work within the setting of a constituent quark model. The kind of processes we are interested in, such as $M + \nu_e \to M' + e$ for example, shall be investigated for momentum transfers up to several GeV. Therefore the need of a relativistically invariant description is obvious. According to P.M. Dirac there are three forms of relativistic (quantum) dynamics [Dir49], where the point form is certainly the least exploited. A rather universal formalism to describe the structure of bound few body systems using the point form of relativistic dynamics had been developed over the last decade and had been successfully applied to calculate meson spectra [KSK03] and electroweak meson (transition) form factors [BSFK09, GR11]. The resulting spacelike electromagnetic form factors were comparable to corresponding calculations in front form and to experimental results. The weak decay form factors, however, were found to deviate for higher (timelike) momentum transfers from front-form calculations and also from the sparse experimental data. One possible reason for this discrepancy is suspected to be missing non-valence contributions and their different roles in point form and in front form. The aim of this thesis is to give an estimate for the size of, so called, *Z-graphs*, a specific kind of non-valence contributions, and to check, whether deviations from experimental data shrink after including such graphs. The semileptonic transition of a meson M into a meson M', as it is seen in a simple constituent-quark picture, is depicted on the left-hand side of Fig. 1.1. The right-hand side shows the Z-graph contribution. In principle such contributions are treatable within the kind of approach we are using, by introducing additional channels to account for the extra $q\bar{q}$-pair. But instead

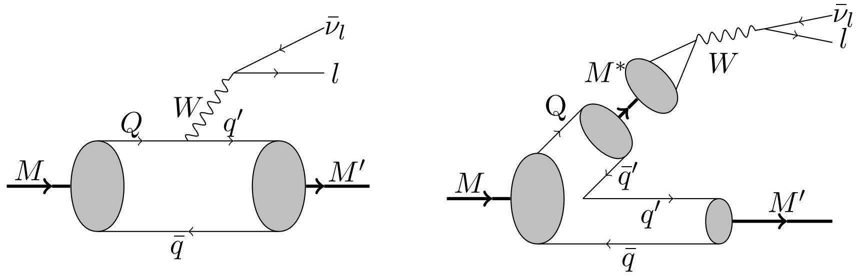

Figure 1.1: Semileptonic decay $M \to M' + l + \bar{\nu}_l$ in a valence-quark picture (left) and the Z-graph contribution to the decay amplitude (right).

of including Z-graphs explicitly we will follow a different approach. Let us first consider lepton-meson scattering. It is obvious that for an infinitely fast moving meson the production of a quark-antiquark pair, and therefore also the contribution of Z-graphs, should be suppressed. This is realized in the infinite-momentum frame where, using Mandelstam variables s and t to parametrize the relativistic kinematics, s approaches infinity. Working in the infinite-momentum frame, however, is not possible for decay kinematics since this would correspond to infinitely large momentum transfer between the initial meson and the outgoing neutrino, or equivalently, infinitely large invariant mass of the outgoing meson and the electron. For the scattering process, on the other hand, we do not face this problem. The idea is now to calculate the transition amplitude for meson-neutrino scattering in the infinite-momentum frame and obtain the decay form factors by analytic continuation of the (spacelike) transition form factors into the timelike momentum-transfer region. This is possible since the scattering amplitude and therefore also the form factors are meromorphic functions of the momentum transfer squared. The formalism presented in the following will be used in Chap. 3 to calculate the 1-W exchange amplitude for meson-neutrino scattering. Meson-neutrino scattering will be treated as a coupled-channel problem with instantaneously confined constituent quarks and the W showing up as a dynamical degree-of-freedom. Relativistic invariance is ensured by using the Bakamjian-Thomas construction [BT53] and the interaction with the lepton is treated perturbatively by dynamical W-boson exchange. Then, by analyzing the structure of the scattering amplitude, we can identify the bound-state current in a unique way. In Chap. 4 we present the form factors for spacelike momentum transfer, obtained by a covariant decomposition of the bound-state current. This will be done in two specific frames of reference. The infinite-momentum frame, where the invariant mass squared of the incoming particles approaches infinity, and the Breit-frame of reference, which corresponds to backward scattering. In this context we will discuss a fundamental problem, namely violation of macrocausality or cluster separability. Cluster separability means that two subsystems become independent of each other, if they are separated by a sufficiently large spacelike distance. This is a problem one faces in every form of relativistic dynamics when using the Bakamjian-Thomas construction and going beyond the pure two-particle problem [KP91]. The discussion of the analytic continuation and the comparison with direct decay calculations, where Z-graphs are not taken into account, follow in Chap. 5. There we will also present a parametrization of the calculated form factors and discuss a vector-meson-dominance like mechanism that accounts effectively for Z-graphs. To complete the picture, the influence of Z-graphs on heavy-quark symmetry and heavy-quark symmetry breaking is discussed in Chap. 6. The diploma thesis will end with a summary and an outlook.

Chapter 2

Theoretical Framework

To set up the theoretical framework which this work is based on, we will proceed as follows: First we will sketch how to formulate a relativistically invariant quantum mechanical model. Although it seems to be trivial, we will start with the Hilbert space for free particles, since it is a convenient point to start from and also a good opportunity to introduce the not so familiar velocity-state representation of the Poincaré group. The next step will be to include interactions into our theory and to set up a coupled-channel formalism to account for particle creation and annihilation as well as dynamical particle exchange. This framework has been developed and extended in previous work, so the present chapter must be seen as recapitulation and summary of the state of the art. For further details we will, of course, refer to the corresponding papers whenever necessary.

2.1 Relativistic Invariance of Free Particles

2.1.1 The Poincaré Group

In order to ensure any kind of invariance of a theory that is represented on a particular Hilbert space, it is necessary to find a (anti)unitary representation of the corresponding symmetry group. In the case of relativistic invariance this symmetry group is the Poincaré group. The Poincaré or inhomogeneous Lorentz group is the group of transformations that preserve proper time τ_{xy} between events in Minkowski space which take place at different points in space-time, x^μ and y^μ, respectively. The transformations which leave the proper time

$$\tau_{xy}^2 := g_{\mu\nu}(x-y)^\mu(x-y)^\nu \tag{2.1}$$

invariant are space-time translations and Lorentz transformations. They have the general form

$$x^\mu \to x'^\mu = \Lambda^\mu{}_\nu x^\nu + a^\mu, \tag{2.2}$$

with $a^\mu \in \mathbb{R}^4$ and $\Lambda \in \mathcal{L} = O(1,3)$. The Lorentz group $\mathcal{L}$ is a Lie-group with a six-dimensional parameter space and can be decomposed into the four components

$$\begin{aligned}
\mathcal{L}_+^\uparrow &\equiv \{\Lambda \in \mathcal{L} | \Lambda^0{}_0 \geq 1, \det\Lambda = +1\}, \\
\mathcal{L}_-^\uparrow &\equiv \{\Lambda \in \mathcal{L} | \Lambda^0{}_0 \geq 1, \det\Lambda = -1\}, \\
\mathcal{L}_-^\downarrow &\equiv \{\Lambda \in \mathcal{L} | \Lambda^0{}_0 \leq 1, \det\Lambda = -1\}, \\
\mathcal{L}_+^\downarrow &\equiv \{\Lambda \in \mathcal{L} | \Lambda^0{}_0 \leq 1, \det\Lambda = +1\},
\end{aligned} \tag{2.3}$$

of which only $\mathcal{L}_+^\uparrow$ is a real subgroup, because only this component contains $\mathbb{1}_4$, the neutral element of the group. For this reason $\mathcal{L}_+^\uparrow$ is called the proper orthochronous Lorentz group. Since all four components can be constructed by applying an element of the discrete Lorentz subgroup, the Klein group, which consists of parity transformation P, time reversal T, four-dimensional reflection PT and the unity in four-dimensional real space $\mathbb{1}_4$, on the proper orthochronous Lorentz group

$$\begin{aligned}
\mathcal{L}_+^\uparrow &= \mathbb{1}_4 \mathcal{L}_+^\uparrow, \\
\mathcal{L}_-^\uparrow &= P\mathcal{L}_+^\uparrow, \\
\mathcal{L}_-^\downarrow &= T\mathcal{L}_+^\uparrow, \\
\mathcal{L}_+^\downarrow &= PT\mathcal{L}_+^\uparrow,
\end{aligned} \tag{2.4}$$

we will concentrate on these two subgroups instead of dealing with $\mathcal{L}$ itself. See, for example, [SW64] for further details. The proper Poincaré group $\mathcal{P}_+^\uparrow$ is then the semidirect product of $\mathcal{L}_+^\uparrow$ and the group of four-dimensional translations. Therefore its parameter space is 10 dimensional. Three parameters belong to the three-vector $\mathbf{\Theta}$ describing rotations in three-dimensional Euclidean space, another three form the three-velocity $\mathbf{v}$, which parametrizes a canonical boost, and the remaining four parameters can be combined to the four-vector a which describes space-time translations. Each parameter is connected with one one-parameter subgroup of the proper Poincaré group and a corresponding infinitesimal generator. The corresponding ten generators of the Poincaré group are:

- P^μ, $\mu = 0, 1, 2, 3 \cdots$ generators of space-time translations,
- K^j, $j = 1, 2, 3 \cdots$ generators of Lorentz boosts in all spatial directions,
- J^j, $j = 1, 2, 3 \cdots$ generators of rotations in three-dimensional Euclidean space.

The Lie-algebra of the group can then be expressed in commutator relations which the generators have to satisfy. For the generators of the Poincaré group, the algebra reads

$$
\begin{aligned}
[P^\mu, P^\nu] &= 0, \\
[P^i, J^j] &= \imath\epsilon^{ijk} P^k, \\
[P^0, J^j] &= 0, \\
[P^i, K^j] &= \imath\delta^{ij} P^0, \\
[P^0, K^j] &= \imath P^j, \\
\\
[J^i, J^j] &= \imath\epsilon^{ijk} J^k, \\
[K^i, J^j] &= \imath\epsilon^{ijk} K^k, \\
[K^i, K^j] &= -\imath\epsilon^{ijk} J^k.
\end{aligned}
\tag{2.5}
$$

The three boost-generators K^j and the generator of spatial rotations J^j can be combined to one total antisymmetric tensor of rank 2, $M^{\mu\nu}$:

$$
\begin{aligned}
M^{0i} &= K^i \ldots i = 1, 2, 3, \\
M^{ij} &= \epsilon^{ijk} J^k, \\
M^{\mu\nu} &= -M^{\nu\mu}.
\end{aligned}
\tag{2.6}
$$

The Poincaré algebra can then be written in manifest covariant form

$$
\begin{aligned}
[P^\mu, P^\nu] &= 0, \\
[M^{\mu\nu}, P^\sigma] &= \imath(g^{\nu\sigma} P^\mu - g^{\mu\sigma} P^\nu), \\
[M^{\mu\nu}, M^{\sigma\rho}] &= -\imath(g^{\mu\sigma} M^{\nu\rho} - g^{\nu\sigma} M^{\mu\rho} + g^{\nu\rho} M^{\mu\sigma} - g^{\mu\rho} M^{\nu\sigma}).
\end{aligned}
\tag{2.7}
$$

As mentioned at the beginning of this section, the aim is to construct a unitary representation of the Poincaré group, acting on the considered Hilbert space. Since $P_+^\uparrow$ has no simply connected topology, because it contains the

group $SO(3) \cong SU(2)/\mathbb{Z}_2$ which has no simply connected parameter space, we are instead looking for a unitary representation of the universal covering group. Following Wigner's and Bergmann's theorems (see, e.g., [Tha92]) the representation of a connected Lie group can be constructed from the unitary representation of its universal covering group. The covering group of the proper orthochronous Poincaré group is the inhomogeneous $SL(2,\mathbb{C})$, which is the group of ordered pairs of complex (2×2) matrices $(\underline{\Lambda}, \underline{a})$ with $\det\underline{\Lambda} = 1$ and $\underline{a} = \underline{a}^\dagger$. Here we have adopted the notation used in [Biernat11] to distinguish between elements (Λ, a) of the Poincaré group and elements $(\underline{\Lambda}, \underline{a})$ which belong to the universal covering group. To illustrate the correspondence of $ISL(2,\mathbb{C})$ and $P_+^\uparrow$ we will shortly repeat the construction of Refs. [KP91] and [Tha92].
Every space-time coordinate x^μ with $x \in \mathbb{R}^4$ can be represented by a hermitian 2×2 matrix

$$\sigma(x) = \sum_{\mu=0}^{3} x^\mu \sigma_\mu, \tag{2.8}$$

with $\sigma_i \ldots i = 1, 2, 3$ being the Pauli matrices and σ_0 being the identity matrix in $\mathbb{R}^2$. The proper time defined in Eq. (2.1) can then be expressed by the determinant

$$\tau_{xy}^2 = \det[\sigma(x) - \sigma(y)]. \tag{2.9}$$

If we define the action of $(\underline{\Lambda}, \underline{a})$ on $\sigma(x)$ by

$$(\underline{\Lambda}, \underline{a}) : \sigma(x) \to \sigma'(x) = \underline{\Lambda}\sigma(x)\underline{\Lambda}^\dagger + \underline{a}, \tag{2.10}$$

one can show that all transformations of this form preserve the proper time, Eq. (2.9), and form a group under the composition

$$(\underline{\Lambda}_2, \underline{a}_2) \circ (\underline{\Lambda}_1, \underline{a}_1) := (\underline{\Lambda}_2\underline{\Lambda}_1, \underline{\Lambda}_2\underline{a}_1\underline{\Lambda}_2^\dagger + \underline{a}_2), \tag{2.11}$$

with the inverse element $(\underline{\Lambda}, \underline{a})^{-1} = (\underline{\Lambda}^{-1}, -\underline{\Lambda}^{-1}\underline{a}(\underline{\Lambda}^\dagger)^{-1})$. Because $ISL(2,\mathbb{C})$ is the universal covering group and therefore has a simply connected parameter space, it is clear that the homomorphisms $SL(2,\mathbb{C}) \to P_+^\uparrow$ must posses a nontrivial kernel. In fact always two elements of $SL(2,\mathbb{C})$, namely $(\underline{\Lambda}, \underline{a})$ and $(-\underline{\Lambda}, \underline{a})$ correspond to the same element (Λ, a) of $P_+^\uparrow$. As a consequence, $P_+^\uparrow$ is isomorphic to the factor group with respect to the kernel of the homomorphism $P_+^\uparrow \cong (SL(2,\mathbb{C})/\mathbb{Z}_2) \odot \mathbb{R}^4$, where $\odot$ denotes the semidirect product. As a remark it should be mentioned that so far we have constructed a two-dimensional representation of $P_+^\uparrow$. To cover the full Poincaré group, remembering the decomposition Eq. (2.4), we have to include the discrete Lorentz group. As it is shown in [Tha92] the parity transformation is an automorphism of the $SL(2,\mathbb{C})$ onto itself that cannot be represented by $SL(2,\mathbb{C})$ matrices. Instead the dimension of the representation has to be doubled. The covering group of the full Poincaré group is then obtained by building the semidirect product of $\mathbb{R}^4$ and $\tilde{\mathcal{L}}$, where

$$
\begin{aligned}
\tilde{\mathcal{L}} &\equiv \{\mathbf{L_A}, \mathbf{L_P L_A}, \mathbf{L_T L_A}, \mathbf{L_P L_T L_A} | \mathbf{A} \in \mathbf{SL(2,\mathbb{C})}\}\,, \\
\mathbf{L_A} &\equiv \begin{pmatrix} \mathbf{A} & 0 \\ 0 & (\mathbf{A}^*)^{-\mathbf{1}} \end{pmatrix}, \\
\mathbf{L_P} &\equiv \begin{pmatrix} 0 & \mathbb{1}_2 \\ \mathbb{1}_2 & 0 \end{pmatrix}, \\
\mathbf{L_T} &\equiv \begin{pmatrix} 0 & -\imath\, \mathbb{1}_2 \\ \imath\, \mathbb{1}_2 & 0 \end{pmatrix},
\end{aligned} \tag{2.12}
$$

is the covering group of the full Lorentz group. For a detailed derivation and further discussions of the group-theoretical properties we refer to [Tha92]. Mentioned for mathematical rigor, we restrict our consideration from now on to the part of the Poincaré group which is connected to the identity and the two dimensional representation of its covering group $ISL(2,\mathbb{C})$.

2.1.2 Unitary Representation

To construct a unitary representation of the Poincaré algebra, Eq. (2.5), on a multi-particle Hilbert space we will follow the lines of Ref. [KP91]. Thereby we will adopt the notation used in [Biernat11]. A suitable basis for a one-particle Hilbert space $\mathcal{H}$ consists of the states

$$
|m, j, \mathbf{p}, \sigma\rangle \equiv |\mathbf{p}, \sigma\rangle, \tag{2.13}
$$

which are simultaneous eigenstates of the one-body operators $\hat{m}^2$, $\hat{\mathbf{j}}^2$, $\hat{\mathbf{p}}$ and $\hat{j}_c^3$.

- $\hat{\mathbf{p}}$ is the momentum operator and $\hat{p}^i,\ i = 1 \ldots 3$ are the spatial components of the free four-momentum operator.
- $\hat{m}^2$ is the mass operator and one of the two Casimir operators for the representation, $\hat{m}^2 := \hat{p}^\mu \hat{p}_\mu$.
- $\hat{\mathbf{j}}^2$ is the square of the (total) angular momentum operator and the second Kasimir operator.

- $\hat{j}_c^3$ is the three-component of the (total) angular momentum operator.

The operators $\hat{p}^\mu$ and $\hat{j}^j$ are the generators of space-time translations and three-dimensional rotations on the one-particle Hilbert space and fulfill the commutator relations, Eq. (2.5). The representation $\hat{U}(\underline{\Lambda}, \underline{a})$ of the proper Poincaré group on the one-particle Hilbert space spanned by the states $|\mathbf{p}, \sigma\rangle$ is given by

$$\hat{U}(\underline{\Lambda}, \underline{a})|\mathbf{p}, \sigma\rangle = \mathrm{e}^{-\imath(\Lambda\ p)\cdot a} \sum_{\sigma'=-j}^{j} D^j_{\sigma'\sigma}[\underline{R}_{W_c}(v, \Lambda)]|\mathbf{\Lambda p}, \sigma'\rangle, \tag{2.14}$$

where $\mathbf{\Lambda p}$ denotes the spatial components of the four-momentum after applying the Lorentz transformation Λ. The matrix elements $D^j_{\sigma'\sigma}[\underline{R}_{W_c}(v, \Lambda)]$ are the Wigner D-functions which correspond to a $2j+1$ dimensional representation of $SU(2)$. The argument of the Wigner D-functions $\underline{R}_{W_c}(v, \Lambda)$ is a Wigner rotation defined via a canonical (rotationless) Lorentz boost $B_c(v)$

$$R_{W_c}(p, \Lambda) := B_c^{-1}(\mathbf{\Lambda p})\Lambda B_c(\mathbf{p}). \tag{2.15}$$

The n-particle Hilbert space is then realized as a tensor product of n single-particle Hilbert spaces $\mathcal{H}_i$

$$\mathcal{H}_{1\ldots n} = \mathcal{H}_1 \otimes \mathcal{H}_2 \otimes \ldots \otimes \mathcal{H}_n. \tag{2.16}$$

A basis for the multi-particle Hilbert space can then be defined in a straight forward manner as tensor product of single particle basis states

$$|\mathbf{p}_1, \sigma_1; \mathbf{p}_2, \sigma_2; \ldots; \mathbf{p}_n, \sigma_n\rangle := |\mathbf{p}_1, \sigma_1\rangle \otimes |\mathbf{p}_2, \sigma_2\rangle \otimes \ldots \otimes |\mathbf{p}_n, \sigma_n\rangle. \tag{2.17}$$

The mass and four-momentum operators acting on this tensor-product Hilbert space read

$$\begin{aligned}
\hat{M}_n &:= \hat{m}_1 \otimes \mathbb{1}_2 \otimes \ldots \otimes \mathbb{1}_n \oplus \mathbb{1}_1 \otimes \hat{m}_2 \otimes \ldots \otimes \mathbb{1}_n \\
&\quad \oplus \ldots \oplus \mathbb{1}_1 \otimes \mathbb{1}_2 \otimes \ldots \otimes \hat{m}_n, \\
\hat{P}_n^\mu &:= \hat{p}_1^\mu \otimes \mathbb{1}_2 \otimes \ldots \otimes \mathbb{1}_n \oplus \mathbb{1}_1 \otimes \hat{p}_2^\mu \otimes \ldots \otimes \mathbb{1}_n \\
&\quad \oplus \ldots \oplus \mathbb{1}_1 \otimes \mathbb{1}_2 \otimes \ldots \otimes \hat{p}_n^\mu.
\end{aligned} \tag{2.18}$$

Also the n-particle unitary representation of the Poincaré group is the tensor product of the irreducible one-particle representations

$$\hat{U}_{12\ldots n}[\underline{\Lambda}, \underline{a}] := \hat{U}_1[\underline{\Lambda}, \underline{a}] \otimes \hat{U}_2[\underline{\Lambda}, \underline{a}] \otimes \ldots \otimes \hat{U}_n[\underline{\Lambda}, \underline{a}]. \tag{2.19}$$

It is a reducible representation with transformation properties following from the transformation properties of the single-particle representations, Eq. (2.14),

$$\hat{U}_{12\ldots n}[\underline{\Lambda}, \underline{a}]|\mathbf{p}_i, \sigma_i\rangle = \mathrm{e}^{-\imath(\Lambda P_n)\cdot a} \sum_{\sigma_i'} |\mathbf{\Lambda p_i}, \sigma_i'\rangle \prod_{i=1}^{n} D^{j_i}_{\sigma_i'\sigma_i}[\underline{R}_{W_c}(v, \Lambda)]. \tag{2.20}$$

$|\mathbf{p}_i, \sigma_i\rangle$ is a short-hand notation for $|\mathbf{p}_1, \sigma_1; \mathbf{p}_2, \sigma_2; \ldots; \mathbf{p}_n, \sigma_n\rangle$ and $\mathbf{\Lambda p_i}$ denotes the spatial components of the four-momentum p_i after applying a Lorentz transformation Λ. $P_n = \sum_{i=1}^{n} p_i$ is the total four-momentum of the system.

2.1.3 Velocity States

Although the basis states considered in the last section are the common choice for the multi-particle Hilbert space, we will use another complete set of states that is more suitable for the Bakamjian-Thomas construction carried out in the point form of relativistic dynamics. These states are called "velocity states" and had been introduced by W. H. Klink in [Kli98]. Let us assume an n-particle state with particle i having momentum $\mathbf{k}_i$. If the whole system is at rest the particle momenta have to satisfy

$$\sum_{i=1}^{n} \mathbf{k}_i = 0. \tag{2.21}$$

A velocity state is then obtained by boosting the whole system with momenta $\mathbf{k}_i$ and spin projections μ_i to an overall velocity V

$$\begin{aligned}
&\hat{U}_{12\ldots n}[\underline{\Lambda}_{B_c(V)}, \underline{a} = 0]|\mathbf{k}_1, \sigma_1; \mathbf{k}_2, \sigma_2; \ldots; \mathbf{k}_n, \sigma_n\rangle \equiv \\
&\hat{U}_{12\ldots n}[\underline{B}_c(V)]|\{\mathbf{k}_i, \mu_i\}\rangle = \sum_{\{\sigma_i\}} |\{\mathbf{p}_i, \sigma_i\}\rangle \prod_{i=1}^{n} D^{j_i}_{\sigma_i\mu_i}[\underline{R}_{W_c}(v_i, B_c(\mathbf{V}))] \\
&:= |V; \mathbf{k}_1, \sigma_1; \mathbf{k}_2, \sigma_2; \ldots; \mathbf{k}_n, \sigma_n\rangle,
\end{aligned} \tag{2.22}$$

with

- $\mathbf{k}_i$, μ_i ... momentum and spin-projection of the i-th particle in the overall rest frame,
- $\mathbf{p}_i$, σ_i ... physical momentum and spin-projection of the i-th particle,
- $v_i := \frac{k_i}{m_i}$ ... four-velocity of the i-th particle in the overall rest frame.

The action of Lorentz transformations is then given by

$$\hat{U}_{12\ldots n}(\underline{\Lambda})|V;\{\mathbf{k}_i,\mu_i\}\rangle = \sum_{\{\mu_i'\}} |\Lambda V;\{\mathbf{R_{W_c}}(\mathbf{V},\mathbf{\Lambda})\mathbf{k_i},\mu_i'\}\rangle \prod_{i=1}^{n} D^{j_i}_{\mu_i',\mu_i}[\underline{W_c}(V,\Lambda)], \tag{2.23}$$

see for example [Kli98] or [Biernat11]. The integration measure and therefore also the completeness relation for n-particle states can be transformed from physical momenta to velocity states. This is done in [Kra01] and the results are summarized in [Biernat11], which shall be repeated shortly. The completeness relation for n-particle tensor-product states reads

$$\hat{1}_{\{n\}} = \sum_{\{\mu_i\}} \int \prod_{i=1}^{n} \frac{d^3 p_i}{(2\pi)^3 2p_i^0} |\{\mathbf{p}_i,\sigma_i\}\rangle\langle\{\mathbf{p}_i,\sigma_i\}|. \tag{2.24}$$

Using the transformed integration measure

$$\int \prod_{i=1}^{n} \frac{d^3 p_i}{2p_i^0} = \int \frac{d^3 V}{V^0} \left(\prod_{i=1}^{n-1} \frac{d^3 k_i}{2k_i^0}\right) \frac{\left(\sum_{j=1}^{n} k_j^0\right)^3}{2k_n^0}, \tag{2.25}$$

the corresponding completeness relation for velocity states becomes

$$\hat{1}_n = \sum_{\{\mu_i\}} \int \frac{d^3 V}{(2\pi)^3 V_0} \left(\prod_{i=1}^{n-1} \frac{d^3 k_i}{(2\pi)^3 2k_i^0}\right) \frac{(\sum_{i=1}^{n} k_i^0)^3}{2k_n^0} |V;\{\mathbf{k}_i,\mu_i\}\rangle\langle V;\{\mathbf{k}_i,\mu_i\}|. \tag{2.26}$$

Therefore the velocity states have to fulfill the orthogonality relation

$$\begin{aligned} \langle V';\{\mathbf{k}_i',\mu_i'\}|V;\{\mathbf{k}_i,\mu_i\}\rangle &= V_0 \delta^3(\mathbf{V'}-\mathbf{V}) \frac{(2\pi)^3 2k_n^0}{(\sum_{i=1}^{n} k_i^0)^3} \\ &\times \left(\prod_{i=1}^{n-1} (2\pi)^3 2k_i^0 \delta^3(\mathbf{k}_i'-\mathbf{k}_i)\right) \prod_{i=1}^{n} \delta_{\mu_i'\mu_i}. \end{aligned} \tag{2.27}$$

2.2 Relativistic Invariance of Interacting Particles

So far we have constructed a unitary representation of the proper orthochronous Poincaré group for an interaction-free n-particle system on a pertinent Hilbert space. The unitarity of the representation ensures relativistic invariance of our description of freely moving particles. Our next goal is to extend this construction in such a way that interactions can be included. B. Bakamjian and L. H. Thomas provided a consistent prescription of doing so [BT53]. This, so called, "Bakamjian-Thomas construction" will be discussed in the following.

2.2.1 The Point Form of Relativistic Quantum Mechanics

If one deals with an interacting system interaction terms show up in the Hamiltonian $\hat{P}^0$. Since

$$[P^i, K^j] = \imath\, \delta^{ij} P^0,$$

it is unavoidable that also other Poincaré generators will be affected by the interaction. P. A. M. Dirac introduced three different forms of relativistic dynamics which are specified by the interaction independent Poincaré subgroups [Dir49], the "instant form", the "front form" and the "point form". In the instant form the interaction dependent generators, which are also called "dynamical" generators or "Hamiltonians", are P^0, K^1, K^2 and K^3 and the interaction independent or "kinematic" generators are therefore P^1, P^2, P^3, the generators of spatial translations, and J^1, J^2 and J^3, the generators of rotations. The term "instant form" refers to the hypersurface of Minkowski space which is left invariant under the kinematic subgroup generated by the kinematic generators, in this case the instant $x^0 = 0$. The hypersurface which is left invariant in the front form is the light front $x^0 + x^3 = 0$. In this form only three generators are dynamical, namely $P^0 - P^3$, $K^1 - J^2$ and $K^2 + J^1$, which is less than in any other form. The third and also least known form is the "point form" of relativistic dynamics with the Lorentz group being the kinematic group, leaving not only the "point" $x^\mu = 0$, but also the hyperboloid $x^\mu x_\mu = 0$ invariant. Since the generators of the Lorentz group are interaction independent, standard SU(2) Clebsch-Gordan coefficients can be used to add angular momentum and spin. With the components of the four-momentum operator P^μ containing all interactions one has only to worry about the first two commutation relations in Eq. (2.7) when including interactions. This leads to the, so called, "point-form equations"

$$\begin{aligned}&[P^\mu, P^\nu] = 0,\\ &\hat{U}(\underline{\Lambda})P^\mu\hat{U}^\dagger(\underline{\Lambda}) = (\Lambda^{-1})^\mu{}_\nu P^\nu.\end{aligned} \tag{2.28}$$

2.2.2 Bakamjian-Thomas Construction

The general idea of Bakamjian and Thomas was to start with the generators corresponding to the non-interacting multi-particle representation and construct a set of auxiliary operators. This set depends on the specific form of dynamics. In point form the auxiliary operators are the free mass operator $\hat{M}_n^{\mathrm{free}}$, the free velocity operator $\hat{V}^\mu_{\mathrm{free}}$ and the generators of the Lorentz group $\hat{K}_n^j$ and $\hat{J}_n^j$, where the mass and four-velocity operators are constructed according to

$$\hat{M}_{\mathrm{free}} = \sqrt{\hat{P}^\mu_{\mathrm{free}}\hat{P}^{\mathrm{free}}_\mu}, \tag{2.29}$$

$$\hat{V}^\mu_{\mathrm{free}} = \frac{\hat{P}^\mu_{\mathrm{free}}}{\hat{M}_{\mathrm{free}}}. \tag{2.30}$$

An interaction term is then added to the mass operator only and the original set of operators is reconstructed.

$$\hat{M} = \hat{M}_{\mathrm{free}} + \hat{M}_{\mathrm{int}}, \tag{2.31}$$

$$\hat{P}^\mu = (\hat{M}_{\mathrm{free}} + \hat{M}_{\mathrm{int}})\hat{V}^\mu_{\mathrm{free}}. \tag{2.32}$$

The algebra, Eq. (2.5), implies constraints on the interaction term added to the mass operator, namely that its commutator with all other auxiliary operators vanishes:

$$[\hat{M}_{\mathrm{int}}, \hat{V}^\mu] = [\hat{M}_{\mathrm{int}}, \hat{K}^j] = [\hat{M}_{\mathrm{int}}, \hat{J}^j] = 0. \tag{2.33}$$

By satisfying these constraints for the interaction term, one obtains an interacting representation of the Poincaré group on a multi-particle Hilbert space. Notable, this construction allows even to include instantaneous interactions in a relativistically invariant manner.

2.2.3 Instantaneous Quark-Antiquark Interaction

We have just seen how to introduce an instantaneous interaction into a quantum mechanical theory in such a way that Poincaré invariance is ensured.

What we need to know in the following is how two-body interactions are defined in a three- or four-particle Hilbert space. Therefore we will start with a two-particle Hilbert space and use a two-particle basis which consists of states that transform irreducibly under $(2j+1)$-dimensional representations of $SU(2)$. This means a change of basis from tensor products of single-particle states of the form (2.22) to two particle states $|\mathbf{k}_{12}; \tilde{k}; j, \mu_j\rangle$, with

- $\mathbf{k}_{12}$ ... total three-momentum of the two particles,
- $\tilde{k}$ ... magnitude of the three-momentum of particle 1 in the rest frame of the two-particle system (equals half the relative momentum)[1],
- j ... total (canonical) spin of the two-particle system,
- μ_j ... spin projection of the two-particle system.

The way how to construct this transformation explicitly is shown in [Pol09], [KP91], [Biernat11] and only the result will be stated here:

$$\begin{aligned}
&\langle \mathbf{k}_{12}; \tilde{k}; j, \mu_j | \mathbf{k}_1, \mu_1; \mathbf{k}_2, \mu_2 \rangle \\
= \;& (2\pi)^6 \int_\Omega d\Omega(\tilde{\mathbf{k}}) 2k_{12}^0 \delta^3(\mathbf{k}_{12} - \mathbf{k}_1 - \mathbf{k}_2) \frac{2\tilde{k}_1^0 2\tilde{k}_2^0}{2m_{12}} \delta^3(\tilde{\mathbf{k}} - \mathbf{B}_c^{-1}(\boldsymbol{\omega}_{12}) k_1) Y^*_{l\mu_l}(\tilde{\mathbf{k}}) \\
& \times C^{s\mu_s}_{j_1\tilde{\mu}_1 j_2\tilde{\mu}_2} C^{j\mu_j}_{l\mu_l s\mu_s} D^{j_1}_{\tilde{\mu}_1\mu_1}[\underline{R}^{-1}_{W_c}(\tilde{\omega}_1, \mathbf{B}_c(\boldsymbol{\omega}_{12}))] D^{j_2}_{\tilde{\mu}_2\mu_2}[\underline{R}^{-1}_{W_c}(\tilde{\omega}_2, \mathbf{B}_c(\boldsymbol{\omega}_{12}))].
\end{aligned} \tag{2.34}$$

m_{12} is the invariant mass of the two particle system. $\tilde{\omega}_i$ and $\boldsymbol{\omega}_{12}$ denote the velocity of particle i in the center-of-momentum frame and the three-velocity of the two-particle system, respectively.
If we now include a term which provides the interaction between the two particles, $\hat{M}_C = \hat{M}_{12}^{\text{free}} + \hat{M}_{\text{int}}$, the Bakamjian-Thomas constraints on the interacting part imply that the matrix elements of $\hat{M}_{\text{int}}$ between states of an irreducible $(2j+1)$-dimensional representation are of the form [Biernat11]

$$\begin{aligned}
&\langle \mathbf{k}'_{12}; \tilde{k}'; (l', s'), j' \mu'_j | \hat{M}_{\text{int}} | \mathbf{k}_{12}; \tilde{k}; (l, s), j, \mu_j \rangle \\
&= \delta_{jj'} \delta_{\mu_j \mu'_j} (2\pi)^3 2k_{12}^0 \delta^3(\mathbf{k}_{12} - \mathbf{k}'_{12}) \langle \tilde{k}'; l', s' | \hat{M}_{\text{int}} | \tilde{k}; l, s \rangle.
\end{aligned} \tag{2.35}$$

Up to this point there is no difference to the Bakamjian-Thomas construction in instant form. We have constructed the interacting mass operator $\hat{M}_C$

[1]When dealing with 3 or more particles the tilde always indicates the particle momenta in the center-of-momentum frame of the 12-subsystem, i.e. $\tilde{\mathbf{k}}_1 = -\tilde{\mathbf{k}}_2 = \tilde{\mathbf{k}}$.

in such a way that it satisfies the same commutation relations with the auxiliary operators mentioned in Sec. 2.2.2 as the free mass operator $\hat{M}^{\text{free}}$. As a consequence the commuting set of operators $\hat{M}_C^2, \hat{\mathbf{k}}_{12}, \hat{\mathbf{j}}_C^2, \hat{j}_c^3$, with $\hat{\mathbf{j}}_C$ denoting the operator for the canonical spin [KP91, Biernat11], can also be used to label the solution of the mass eigenvalue equation

$$(\hat{M}_{12}^{\text{free}} + \hat{M}_{\text{int}})|\Psi_C\rangle = m_n|\Psi_C\rangle. \tag{2.36}$$

The solutions are of the form $|\mathbf{k}_{12}; n, j, \mu_j\rangle$ with n labeling the discrete eigenvalues of $\hat{M}_C$.[2] It is now obvious that the projection of eigenstates of $\hat{M}_C$ onto eigenstates of the free mass operator $\hat{M}_{12}^{\text{free}}$ is of the form

$$\langle \mathbf{k}'_{12}; \tilde{k}'; (l', s'), j', \mu'_j|\mathbf{k}_{12}, n, j, \mu_j\rangle = N_2\delta(\mathbf{k}_{12} - \mathbf{k}'_{12})\delta_{jj'}\delta_{\mu_j\mu'_j}u^j_{nl's'}(\tilde{k}'), \tag{2.37}$$

with N_2 being a normalization factor. Inserting a complete set of two-particle momentum states (2.24) and using Eq. (2.34) leads to the scalar product

$$\langle \mathbf{k}'_1, \mu'_1; \mathbf{k}'_2, \mu'_2|\mathbf{k}_{12}; n, j, \mu_j\rangle = \tilde{N}_2\delta^3(\mathbf{k}_{12} - \mathbf{k}'_1 - \mathbf{k}'_2)\Psi_{nj\mu_j\mu'_1\mu'_2}(\tilde{\mathbf{k}}'), \tag{2.38}$$

where the two-body bound-state wave function is defined by

$$\begin{aligned}\Psi_{nj\mu_j\mu'_1\mu'_2}(\tilde{\mathbf{k}}') := \quad & \sum_{ls\mu_l\mu_s\tilde{\mu}_1\tilde{\mu}_2} Y_{l\mu_l}(\hat{\tilde{\mathbf{k}}}')C^{s\mu_s}_{j_1\tilde{\mu}_1j_2\tilde{\mu}_2}C^{j_2}_{l\mu_ls\mu_s}u^j_{nls}(\tilde{k}') \\ & \times D^{j_1}_{\mu'_1\tilde{\mu}_1}[\underline{R}_{W_c}(\tilde{\omega}'_1, \mathbf{B}_c(\boldsymbol{\omega}'_{12}))]D^{j_2}_{\mu'_2\tilde{\mu}_2}[\underline{R}_{W_c}(\tilde{\omega}'_2, \mathbf{B}_c(\boldsymbol{\omega}'_{12}))].\end{aligned} \tag{2.39}$$

The next step is to embed the above defined two-body interaction in a three- and four-body Hilbert space. Let us assume that particles 1 and 2 interact via $\hat{M}_{12}^{\text{int}}$, whereas l, a lepton, and W, the gauge boson, act as spectators. Following [Biernat11] and [KSK03] this leads to scalar products

$$\begin{aligned} & \langle V'; \mathbf{k}'_1, \mu'_1; \mathbf{k}'_2, \mu'_2; (\mathbf{k}'_l), \mu'_l|V; \mathbf{k}_{12}, n, j, \mu_j; (\mathbf{k}_l), \mu_l\rangle \\ = \quad & N_3V'^{\,0}\delta^3(\mathbf{V}' - \mathbf{V})\delta_{\mu'_l\mu_l}\delta^3(\mathbf{k}'_l - \mathbf{k}_l)\Psi_{nj\mu_j\mu'_1\mu'_2}(\tilde{\mathbf{k}}')\end{aligned} \tag{2.40}$$

and

$$\begin{aligned} & \langle V'; \mathbf{k}'_1, \mu'_1; \mathbf{k}'_2, \mu'_2; (\mathbf{k}'_W), \mu'_W; \mathbf{k}'_l, \mu'_l|V; \mathbf{k}_{12}, n, j, \mu_j; (\mathbf{k}_W), \mu_W; \mathbf{k}_l, \mu_l\rangle \\ = \quad & N_4V'^{\,0}\delta^3(\mathbf{V}' - \mathbf{V})(-g^{\mu'_W\mu_W})\delta_{\mu'_l\mu_l}\delta^3(\mathbf{k}'_W - \mathbf{k}_W) \\ & \times\delta^3(\mathbf{k}'_l - \mathbf{k}_l)\Psi_{nj\mu_j\mu'_1\mu'_2}(\tilde{\mathbf{k}}')\end{aligned} \tag{2.41}$$

[2] We are mainly thinking of $\hat{M}_{\text{int}}$ being a confining quark-antiquark interaction

which define the two-body bound-state wavefunction in the three- and four-body Hilbert spaces.

2.3 Coupled-Channel Approach

In this work weak interactions are treated in a perturbative way and we restrict our considerations on one-particle-exchange processes. We do this in a relativistically invariant manner and in such a way that retardation effects are fully taken into account. Therefore we use a multichannel framework in which a multichannel matrix mass operator $\hat{M}$ acts on a truncated Fock-space (direct sum over a finite number of Hilbert spaces) $\mathcal{H}_N \oplus \mathcal{H}_{N+1} \oplus \ldots \oplus \mathcal{H}_M$. The dynamics of the theory is then described by the mass eigenvalue equation

$$\hat{M} \begin{pmatrix} |\Psi_N\rangle \\ |\Psi_{N+1}\rangle \\ \vdots \\ |\Psi_M\rangle \end{pmatrix} = m \begin{pmatrix} |\Psi_N\rangle \\ |\Psi_{N+1}\rangle \\ \vdots \\ |\Psi_M\rangle \end{pmatrix}, \tag{2.42}$$

with

$$\hat{M} = \begin{pmatrix} \hat{M}_N & \hat{K}_{N\to N+1} & \cdots \\ \hat{K}^\dagger_{N\to N+1} & \hat{M}_{N+1} & \cdots \\ \vdots & & \ddots \end{pmatrix}. \tag{2.43}$$

The diagonal entries are mass operators $\hat{M}_N$ containing the sum of the relativistic kinetic energies of the particles and instantaneous two-body interactions as described in Sec. (2.2.3). $\hat{K}_{i\to j} = \hat{K}^\dagger_{j\to i}$, the off-diagonal elements, are called vertex operators. These vertex operators allow for transitions between Hilbert spaces corresponding to different particle numbers and species of particles by particle creation and annihilation:

$$\hat{K}^\dagger_{N\to N+1} : \mathcal{H}_N \to \mathcal{H}_{N+1}. \tag{2.44}$$

A general procedure to construct such vertex operators, which can be used in a Bakamjian Thomas type mass operator, had been developed in [Kli03a] and applied in [Biernat11] and [Fuc07] to describe dynamical photon exchange in an electron-meson system, as well as in [GRS12] to account for W-boson exchange and weak mesonic decays. This formalism will be briefly summarized.

Starting with a quantum-field-theoretical interaction Lagrangian density $\mathscr{L}_{\mathrm{int}}(x)$, the interacting part of the corresponding four-momentum operator is obtained by integrating the interaction density over the quantization surface. Since we are working in point form, which is specified by the space-like forward hyperboloid $x^\mu x_\mu = \tau^2$ being the quantization surface, the interaction part of the four-momentum operator reads

$$\hat{P}^\mu_{\rm int} = -\int 2\ {\rm d}^4x\ \delta(x^\mu x_\mu - \tau^2)\ \Theta(x^0)\ x^\mu\ \hat{\mathscr{L}}_{\rm int}(x). \tag{2.45}$$

This construction preserves the Poincaré algebra, as long as the interaction density transforms like a Lorentz scalar [Kra01]

$$\hat{U}(\Lambda, a)\mathscr{L}_{\rm int}(x)\hat{U}^\dagger(\Lambda, a) = \mathscr{L}_{\rm int}(\Lambda x + a). \tag{2.46}$$

Having the Bakamjian-Thomas construction in mind, which allows to separate the overall four-velocity, we are searching for a velocity-state representation of the vertex operators $\hat{K}_{n\to n+1}$ which should be connected with $P^\mu_{\rm int}$ via

$$\begin{aligned} & \langle \mathbf{V}'; \mathbf{k}'_1, \mu'_1; \cdots; \mathbf{k}'_n, \mu'_n; \mathbf{k}'_{n+1}, \mu'_{n+1} | \hat{P}^\mu_{\rm int} | \mathbf{V}; \mathbf{k}_1, \mu_1; \cdots; \mathbf{k}_n, \mu_n\rangle \\ = \quad & V^\mu \langle \mathbf{V}'; \mathbf{k}'_1, \mu'_1; \cdots; \mathbf{k}'_n, \mu'_n; \mathbf{k}'_{n+1}, \mu'_{n+1} | \hat{K}_{n\to n+1} | \mathbf{V}; \mathbf{k}_1, \mu_1; \cdots; \mathbf{k}_n, \mu_n\rangle, \end{aligned} \tag{2.47}$$

With $\hat{K}_{n\to n+1}$ being diagonal in $V^{(\prime)}$. Using the transformation properties of the interaction density and the velocity states, the matrix elements of the field theoretical interacting momentum operator can be written as

$$\begin{aligned} & \langle \mathbf{V}'; \mathbf{k}'_1, \mu'_1; \cdots; \mathbf{k}'_n, \mu'_n; \mathbf{k}'_{n+1}, \mu'_{n+1} | \hat{P}^\mu_{\rm int} | \mathbf{V}; \mathbf{k}_1, \mu_1; \cdots; \mathbf{k}_n, \mu_n\rangle \\ = \quad & -\langle V'; \mathbf{k}'_1, \mu'_1; \cdots; \mathbf{k}'_n, \mu'_n; \mathbf{k}'_{n+1}, \mu'_{n+1} | \hat{\mathscr{L}}_{\rm int}(0) | V; \mathbf{k}_1, \mu_1; \cdots; \mathbf{k}_n, \mu_n\rangle \\ & \times \int 2\ {\rm d}^4x\ \delta(x^\mu x_\mu - \tau^2)\ \Theta(x^0)\ x^\mu\ e^{-{\rm i}(\sum k_i'^0 V' - \sum k_i^0 V)\cdot x}. \end{aligned} \tag{2.48}$$

Within the Bakamjian Thomas construction we have to assume that the left-hand side of Eq. (2.48) is diagonal in V and V', which does not hold in general for the quantum field theoretical case. Evaluating, however, the integral for equal four-velocities, $V = V'$ (see [Kli03a]), we observe that we can factor out the four-velocity

$$\begin{aligned} & \langle \mathbf{V}'; \mathbf{k}'_1, \mu'_1; \cdots; \mathbf{k}'_n, \mu'_n; \mathbf{k}'_{n+1}, \mu'_{n+1} | \hat{P}^\mu_{\rm int} | \mathbf{V}; \mathbf{k}_1, \mu_1; \cdots; \mathbf{k}_n, \mu_n\rangle \\ & = V^\mu f(k_i^0, k_j'^{\,0}) \\ & \times \langle \mathbf{k}'_1, \mu'_1; \cdots; \mathbf{k}'_n, \mu'_n; \mathbf{k}'_{n+1}, \mu'_{n+1} | \hat{\mathscr{L}}_{\rm int}(0) | \mathbf{k}_1, \mu_1; \cdots; \mathbf{k}_n, \mu_n\rangle. \end{aligned} \tag{2.49}$$

The factor $f(k_i^0, k_j'^{\,0})$ is, according to [Kli03a] and [Kra01], a known function. Comparing Eq. (2.49) and Eq. (2.47) and keeping in mind that the matrix elements of the vertex operators should be diagonal in the four-velocity, it is suggestive to relate the vertex matrix elements and the field-theoretical interaction density via

$$\begin{aligned}
&\langle \mathbf{V}; \mathbf{k}_1', \mu_1'; \cdots; \mathbf{k}_n', \mu_n'; \mathbf{k}_{n+1}', \mu_{n+1}' | \hat{K}_{n\to n+1} | \mathbf{V}; \mathbf{k}_1, \mu_1; \cdots; \mathbf{k}_n, \mu_n \rangle \\
&= \frac{(2\pi)^3}{\sqrt{(\sum\limits_{i=1}^{n+1} k_i'^0)^3 \; (\sum\limits_{j=1}^{n} k_j^0)^3}} \; V^0 \; \delta^3(\mathbf{V} - \mathbf{V}') \\
&\times \langle \mathbf{k}_1', \mu_1'; \cdots; \mathbf{k}_n', \mu_n'; \mathbf{k}_{n+1}', \mu_{n+1}' | \hat{\mathscr{L}}_{\mathrm{int}}(0) | \mathbf{k}_1, \mu_1; \cdots; \mathbf{k}_n, \mu_n \rangle .
\end{aligned} \tag{2.50}$$

The factor $f(k_i^0, k_i'^{\,0})$ becomes just a kinematic factor that is chosen such that the same procedure applied to the pure kinetic part of the field theory leads to the correct kinetic part of our quantum mechanical model.

Chapter 3

Neutrino-Meson Scattering

In this work, the process we are interested in is the weak transition of a heavy-light into either a heavy-light or a light-light meson. In order to learn something about the inner (parton) structure of such systems, we calculate the transition amplitude, extract the bound-state current and identify transition form factors which encode the meson structure. In[GRS12] this has been done for the situation of semileptonic meson decays. This section will deal with weak transitions for space-like momentum transfer, as probed in neutrino-meson scattering. On the hadronic level, using first order perturbation theory, the weak scattering of a meson and a neutrino is accomplished by the exchange of a single W-boson which transfers charge and changes the quark flavor (see Fig.3.1). The simplest not-point-like structure one can think of in a constituent quark model, is a confined quark antiquark pair building up the meson[1](see Fig. 3.2).

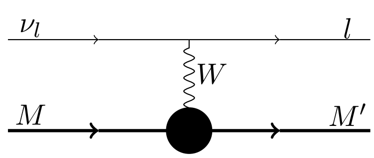

Figure 3.1: Neutrino-meson scattering on the hadronic level

With the framework presented in sections 2.2 and 2.3 we will calculate expressions for the time-ordered contributions which sum up to the covariant scattering amplitude for the process depicted in Fig. 3.2.

[1]The use of upper- and lower-case letters should indicate the heavy-light nature of the incoming meson.

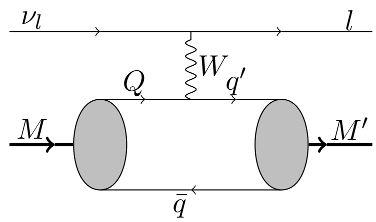

Figure 3.2: Simplest substructure within a CQM as probed in neutrino-meson scattering

3.1 1-W-Exchange Amplitude

To extract the weak $M \to M'$ transition current, we first calculate the invariant 1-W-exchange amplitude. Without loss of generality let us consider the $B^- \nu_e \to D^0 e^-$ scattering process, where the B^- consists of a heavy b and a light $\bar{u}$ quark, whereas the D^0 contains a heavy c and a light $\bar{u}$ quark in our constituent picture.[2] The transition amplitude can be decomposed into two time-ordered graphs shown in Fig. 3.3. Using the coupled-channel approach, the underlying Hilbert space is the direct sum of $\mathcal{H}_{\bar{u}b\nu_e}, \mathcal{H}_{\bar{u}bW^+e}, \mathcal{H}_{\bar{u}ce}$ and $\mathcal{H}_{\bar{u}cW^-\nu_e}$. The matrix mass operator leading to the 1-W-exchange amplitude reads:

$$\hat{M} = \begin{pmatrix} \hat{M}_{\bar{u}b\nu_e} & \hat{K}_{\bar{u}b\nu_e \to \bar{u}bWe} & 0 & \hat{K}_{\bar{u}b\nu_e \to \bar{u}cW\nu_e} \\ \hat{K}^\dagger_{\bar{u}b\nu_e \to \bar{u}bWe} & \hat{M}_{\bar{u}bWe} & \hat{K}_{\bar{u}bWe \to \bar{u}ce} & 0 \\ 0 & \hat{K}^\dagger_{\bar{u}bWe \to \bar{u}ce} & \hat{M}_{\bar{u}ce} & \hat{K}_{\bar{u}ce \to \bar{u}cW\nu_e} \\ \hat{K}^\dagger_{\bar{u}b\nu_e \to \bar{u}cW\nu_e} & 0 & \hat{K}^\dagger_{\bar{u}ce \to \bar{u}cW\nu_e} & \hat{M}_{\bar{u}cW\nu_e} \end{pmatrix}. \quad (3.1)$$

In analogy to Eq.(2.42) the mass eigenvalue equation then reads:

$$\hat{M} \begin{pmatrix} |\Psi_{\bar{u}b\nu_e}\rangle \\ |\Psi_{\bar{u}bWe}\rangle \\ |\Psi_{\bar{u}ce}\rangle \\ |\Psi_{\bar{u}cW\nu_e}\rangle \end{pmatrix} = m \begin{pmatrix} |\Psi_{\bar{u}b\nu_e}\rangle \\ |\Psi_{\bar{u}bWe}\rangle \\ |\Psi_{\bar{u}ce}\rangle \\ |\Psi_{\bar{u}cW\nu_e}\rangle \end{pmatrix}. \quad (3.2)$$

With the help of a Feshbach reduction we eliminate the channels which contain the W. The optical potential which describes the transition between

[2]We emphasize that the presented derivations do not depend on the heavy-light structure of the outgoing meson and all calculations also hold for heavy-light to light-light transitions.

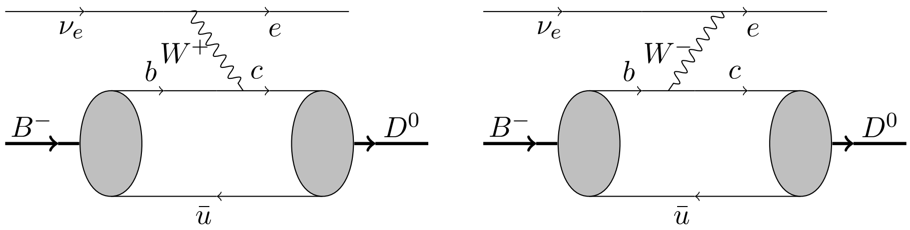

Figure 3.3: Time-ordered graphs contributing to the scattering amplitude for the $B^-\nu_e \to D^0 e^-$ transition.

the two channels we are interested in is then

$$\begin{aligned}\hat{V}_{\mathrm{opt}}^{\bar{u}b\nu_e\to\bar{u}ce}(m) = \quad & \hat{K}_{\bar{u}bWe\to\bar{u}ce}(m-\hat{M}_{\bar{u}bWe})^{-1}\hat{K}^{\dagger}_{\bar{u}bWe\to\bar{u}b\nu_e} \\ + \quad & \hat{K}_{\bar{u}cW\nu_e\to\bar{u}ce}(m-\hat{M}_{\bar{u}cW\nu_e})^{-1}\hat{K}^{\dagger}_{\bar{u}cW\nu_e\to\bar{u}b\nu_e}. \end{aligned} \tag{3.3}$$

Since we are only interested in the Born term for $\nu_e B^- \to e D^0$ scattering we just have to consider on-shell matrix elements ($k_B^0 + k_{\nu_e}^0 = k_D^0 + k_e^0$) of $\hat{V}_{\mathrm{opt}}^{\bar{u}b\nu_e\to\bar{u}ce}$ between eigenstates of $\hat{M}_{\bar{u}b\nu_e}$ and $\hat{M}_{\bar{u}ce}$, respectively:

$$\langle \underline{\mathbf{V}}'; \underline{\mathbf{k}}_D, \underline{\alpha}_D; \underline{\mathbf{k}}_e, \underline{\mu}_e | \hat{V}_{\mathrm{opt}}^{\bar{u}b\nu_e\to\bar{u}ce}(m) | \underline{\mathbf{V}}; \underline{\mathbf{k}}_B, \underline{\alpha}_B; \underline{\mathbf{k}}_{\nu_e}, \underline{\mu}_{\nu_e}\rangle_{\mathrm{o.s}} = \Gamma_1 + \Gamma_2. \tag{3.4}$$

As stated above one gets two time-orderings

$$\begin{aligned}\Gamma_1 \quad = \quad & \langle \underline{\mathbf{V}}'; \underline{\mathbf{k}}_D, \underline{\alpha_D}; \underline{\mathbf{k}}_e, \underline{\mu}_e | \hat{K}_{\bar{u}bWe\to\bar{u}ce}(m-\hat{M}_{\bar{u}bWe})^{-1} \\ & \times \hat{K}^{\dagger}_{\bar{u}bWe\to\bar{u}b\nu_e} | \mathbf{V}; \mathbf{k}_B, \alpha_B; \mathbf{k}_{\nu_e}, \mu_{\nu_e}\rangle_{\mathrm{o.s.}}, \\ \Gamma_2 \quad = \quad & \langle \underline{\mathbf{V}}'; \underline{\mathbf{k}}_D, \underline{\alpha}_D; \underline{\mathbf{k}}_e, \underline{\mu}_e | \hat{K}_{\bar{u}cW\nu_e\to\bar{u}ce}(m-\hat{M}_{\bar{u}cW\nu_e})^{-1} \\ & \times \hat{K}^{\dagger}_{\bar{u}cW\nu_e\to\bar{u}b\nu_e} | \mathbf{V}; \mathbf{k}_B, \alpha_B; \mathbf{k}_{\nu_e}, \mu_{\nu_e}\rangle_{\mathrm{o.s.}}. \end{aligned} \tag{3.5}$$

Because the states $|\underline{\mathbf{V}}'; \underline{\mathbf{k}}_D, \underline{\alpha_D}; \underline{\mathbf{k}}_e, \underline{\mu}_e\rangle$ and $|\mathbf{V}; \mathbf{k}_B, \alpha_B; \mathbf{k}_{\nu_e}, \mu_{\nu_e}\rangle$ are eigenfunctions of the operators $\hat{M}_{\bar{u}ce}$ and $\hat{M}_{\bar{u}b\nu_e}$, respectively, and these operators contain an instantaneous confinement potential, these states are two-body velocity states.[3] To evaluate expression (3.5) we have to insert the appro-

[3]Keep in mind that the momenta $\mathbf{k}_e$ and $\mathbf{k}_{\nu_e}$ are not independent but are fixed through condition (2.21).

priate completeness relations: [4]

$$\begin{aligned}\Gamma_1 = \quad & \langle \underline{\mathbf{V}}'; \underline{\mathbf{k}}_D, \underline{\alpha}_D; \underline{\mathbf{k}}_e, \underline{\mu}_e | \mathbb{1}_{\bar{u}ce} \hat{K}_{\bar{u}bWe\to\bar{u}ce} \mathbb{1}_{\bar{u}bWe} (m - \hat{M}_{\bar{u}bWe})^{-1} \\ & \times \underline{\mathbb{1}}_{\bar{u}bWe} \mathbb{1}_{\bar{u}bWe} \hat{K}^\dagger_{\bar{u}bWe\to\bar{u}b\nu_e} \mathbb{1}_{\bar{u}b\nu_e} | \underline{\mathbf{V}}; \underline{\mathbf{k}}_B, \underline{\alpha}_B; \underline{\mathbf{k}}_{\nu_e}, \underline{\mu}_{\nu_e} \rangle \end{aligned} \tag{3.6}$$

$$\begin{aligned}\Gamma_2 = \quad & \langle \underline{\mathbf{V}}'; \underline{\mathbf{k}}_D, \underline{\alpha}_D; \underline{\mathbf{k}}_e, \underline{\mu}_e | \mathbb{1}_{\bar{u}ce} \hat{K}_{\bar{u}cW\nu_e\to\bar{u}ce} \mathbb{1}_{\bar{u}cW\nu_e} (m - \hat{M}_{\bar{u}cW\nu_e})^{-1} \\ & \times \underline{\mathbb{1}}_{\bar{u}cW\nu_e} \mathbb{1}_{\bar{u}cW\nu_e} \hat{K}^\dagger_{\bar{u}cW\nu_e\to\bar{u}b\nu_e} \mathbb{1}_{\bar{u}b\nu_e} | \underline{\mathbf{V}}; \underline{\mathbf{k}}_B, \underline{\alpha}_B; \underline{\mathbf{k}}_{\nu_e}, \underline{\mu}_{\nu_e} \rangle . \end{aligned} \tag{3.7}$$

Using the completeness relation Eq.(2.26) we obtain for the first time ordering:

$$\begin{aligned}\Gamma_1 = \quad & \sum_{\mu_{\bar{u}}\mu_c\mu_e} \int \frac{d^3V}{(2\pi)^3 V_0} \frac{d^3k_{\bar{u}} d^3k_e}{(2\pi)^6 2k^0_{\bar{u}} 2k^0_e} \frac{(k^0_{\bar{u}} + k^0_c + k^0_e)^3}{2k^0_c} \\
\times \quad & \sum_{\mu'_{\bar{u}}\mu'_b\mu'_W\mu'_e} \int \frac{d^3V'}{(2\pi)^3 V'_0} \frac{d^3k'_{\bar{u}} d^3k'_W d^3k'_e}{(2\pi)^9 2k'^{\,0}_{\bar{u}} 2k'^{\,0}_W 2k'^{\,0}_e} \frac{(k'^{\,0}_{\bar{u}} + k'^{\,0}_W + k'^{\,0}_e + k'^{\,0}_b)^3}{2k'^{\,0}_b} \\
\times \quad & \sum_{\underline{\mu}''_{\bar{u}b}\underline{\mu}''_W\underline{\mu}''_e} \int \frac{d^3\underline{V}''}{(2\pi)^3 \underline{V}''_0} \frac{d^3\underline{k}''_W d^3\underline{k}''_e}{(2\pi)^6 2\underline{k}''^{\,0}_W 2\underline{k}''^{\,0}_e} \frac{(\underline{k}''^{\,0}_{\bar{u}b} + \underline{k}''^{\,0}_W + \underline{k}''^{\,0}_e)^3}{2\underline{k}''^{\,0}_{\bar{u}b}} \\
\times \quad & \sum_{\mu''_{\bar{u}}\mu''_b\mu''_W\mu''_e} \int \frac{d^3V''}{(2\pi)^3 V''_0} \frac{d^3k''_{\bar{u}} d^3k''_W d^3k''_e}{(2\pi)^9 2k''^{\,0}_{\bar{u}} 2k''^{\,0}_W 2k''^{\,0}_e} \frac{(k''^{\,0}_{\bar{u}} + k''^{\,0}_b + k''^{\,0}_e)^3}{2k''^{\,0}_b} \\
\times \quad & \sum_{\mu'''_{\bar{u}}\mu'''_b\mu'''_{\nu_e}} \int \frac{d^3V'''}{(2\pi)^3 V'''_0} \frac{d^3k'''_{\bar{u}} d^3k'''_{\nu_e}}{(2\pi)^6 2k'''^{\,0}_{\bar{u}} 2k'''^{\,0}_{\nu_e}} \frac{(k'''^{\,0}_{\bar{u}} + k'''^{\,0}_b + k'''^{\,0}_{\nu_e})^3}{2k'''^{\,0}_b} \\
\times \quad & \langle \underline{\mathbf{V}}'; \underline{\mathbf{k}}_D, \underline{\alpha}_D; \underline{\mathbf{k}}_e, \underline{\mu}_e | \mathbf{V}; \mathbf{k}_{\bar{u}}, \mu_{\bar{u}}; \mathbf{k}_c, \mu_c \mathbf{k}_e, \mu_e \rangle \\
\times \quad & \langle \mathbf{V}; \mathbf{k}_{\bar{u}}, \mu_{\bar{u}}; \mathbf{k}_e, \mu_e | \hat{K}_{\bar{u}bWe\to\bar{u}ce} | \mathbf{V}'; \mathbf{k}'_{\bar{u}}, \mu'_{\bar{u}}; \mathbf{k}'_b, \mu'_b; \mathbf{k}'_W, \mu'_W; \mathbf{k}'_e, \mu'_e \rangle \\
\times \quad & \langle \mathbf{V}'; \mathbf{k}'_{\bar{u}}, \mu'_{\bar{u}}; \mathbf{k}'_b, \mu'_b; \mathbf{k}'_W, \mu'_W; \mathbf{k}'_e, \mu'_e | \\
& (m - \hat{M}_{\bar{u}bWe})^{-1} | \underline{\mathbf{V}}''; \underline{\mathbf{k}}''_{\bar{u}b}, \underline{\alpha}''_{\bar{u}b}; \underline{\mathbf{k}}''_W, \underline{\mu}''_W; \underline{\mathbf{k}}''_e, \mu''_e \rangle \\
\times \quad & \langle \underline{\mathbf{V}}''; \underline{\mathbf{k}}''_{\bar{u}b}, \underline{\alpha}''_{\bar{u}b}; \underline{\mathbf{k}}''_W, \underline{\mu}''_W; \underline{\mathbf{k}}''_e, \mu''_e | \mathbf{V}''; \mathbf{k}''_{\bar{u}}, \mu''_{\bar{u}}; \mathbf{k}''_b, \mu''_b; \mathbf{k}''_W, \mu''_W; \mathbf{k}''_e, \mu''_e \rangle \\
\times \quad & \langle \mathbf{V}''; \mathbf{k}''_{\bar{u}}, \mu''_{\bar{u}}; \mathbf{k}''_b, \mu''_b; \mathbf{k}''_W, \mu''_W; \mathbf{k}''_e, \mu''_e | \\
& \hat{K}^\dagger_{\bar{u}bWe\to\bar{u}b\nu_e} | \mathbf{V}'''; \mathbf{k}'''_{\bar{u}}, \mu'''_{\bar{u}}; \mathbf{k}'''_b, \mu'''_b; \mathbf{k}'''_{\nu_e}, \mu'''_{\nu_e} \rangle \\
\times \quad & \langle \mathbf{V}'''; \mathbf{k}'''_{\bar{u}}, \mu'''_{\bar{u}}; \mathbf{k}'''_b, \mu'''_b; \mathbf{k}'''_{\nu_e}, \mu'''_{\nu_e} | \underline{\mathbf{V}}; \underline{\mathbf{k}}_B, \underline{\alpha}_B; \underline{\mathbf{k}}_{\nu_e}, \underline{\mu}_{\nu_e} \rangle . \end{aligned} \tag{3.8}$$

The further evaluation of the matrix elements occurring in Eq. (3.8) is done in Secs. 3.1.1 and 3.1.2.

[4] Underlined characters refer to states where two constituents are confined and form a meson

3.1.1 Scalar Products and Wave Functions

In Sec. 2.2.3 we have given a rather general expression for the scalar product between velocity states for free particles and velocity states describing a two-particle bound state. To calculate the transition amplitude from which we are going to extract the bound-state current for neutrino-meson scattering we need explicit expressions for such scalar products. The first scalar product occurring in Eq. (3.8) is the one between the outgoing state containing the D^0 meson and the electron and the free state with the constituents of the D^0 and the electron. According to Eq. (2.40) it can be written as

$$\begin{aligned}&\langle \underline{\mathbf{V}}'; \underline{\mathbf{k}}_D, \underline{\alpha}_D; \underline{\mathbf{k}}_e, \underline{\mu_e} | \mathbf{V}; \mathbf{k}_{\bar{u}}, \mu_{\bar{u}}; \mathbf{k}_c, \mu_c; \mathbf{k}_e, \mu_e \rangle \\ &= N_3 V^0 \delta^3(\mathbf{V} - \underline{\mathbf{V}}') \delta_{\mu_e \underline{\mu_e}} \delta^3(\mathbf{k}_e - \underline{\mathbf{k}}_e) \Psi^*_{\underline{\alpha}_D \mu_{\bar{u}} \mu_c}(\tilde{\mathbf{k}}). \end{aligned} \tag{3.9}$$

Two-particle velocity states are normalized through the condition

$$\begin{aligned}&\langle \underline{\mathbf{V}}'; \underline{\mathbf{k}}_D, \underline{\alpha}_D; \underline{\mathbf{k}}_e, \underline{\mu_e} | \underline{\mathbf{V}}'', \underline{\mathbf{k}}'_D, \underline{\alpha}'_D; \underline{\mathbf{k}}'_e, \underline{\mu_e}' \rangle \\ &= (2\pi)^6 \underline{V}'^{\,0} \delta^3(\underline{\mathbf{V}}' - \underline{\mathbf{V}}'') \delta^3(\underline{\mathbf{k}_e} - \underline{\mathbf{k}}'_e) \delta_{\underline{\mu_e \mu_e}'} \delta_{\underline{\alpha}_D \underline{\alpha}'_D} \frac{2\underline{k_e}^0 2\underline{k}^0_D}{(\underline{k_e}^0 + \underline{k}^0_D)^3}. \end{aligned} \tag{3.10}$$

Inserting the completeness relation for the free states, Eq. (2.26), gives

$$\begin{aligned}&\langle \underline{\mathbf{V}}'; \underline{\mathbf{k}}_D, \underline{\alpha}_D; \underline{\mathbf{k}}_e, \underline{\mu_e} | \mathbb{1}_{\bar{u}ce} | \underline{\mathbf{V}}'', \underline{\mathbf{k}}'_D, \underline{\alpha}'_D; \underline{\mathbf{k}}'_e, \underline{\mu_e}' \rangle \\ &= \sum_{\mu_{\bar{u}} \mu_c \mu_e} \int \frac{d^3V}{(2\pi)^9 V_0} \frac{d^3k_e d^3k_{\bar{u}}}{2k^0_e 2k^0_{\bar{u}}} \frac{(k^0_e + k^0_{\bar{u}} + k^0_c)^3}{2k^0_c} \\ &\times \langle \underline{\mathbf{V}}'; \underline{\mathbf{k}}_D, \underline{\alpha}_D; \underline{\mathbf{k}}_e, \underline{\mu_e} | \mathbf{V}; \mathbf{k}_{\bar{u}}, \mu_{\bar{u}}; \mathbf{k}_c, \mu_c; \mathbf{k}_e, \mu_e \rangle \\ &\times \langle \mathbf{V}; \mathbf{k}_{\bar{u}}, \mu_{\bar{u}}; \mathbf{k}_c, \mu_c; \mathbf{k}_e, \mu_e | \underline{\mathbf{V}}'', \underline{\mathbf{k}}'_D, \underline{\alpha}'_D; \underline{\mathbf{k}}'_e, \underline{\mu_e}' \rangle. \end{aligned} \tag{3.11}$$

As a consequence of Eq. (2.40) and with the transformed integration measure (see [Fuc07])

$$d^3k_{\bar{u}} = d^3\tilde{k}_{\bar{u}} \frac{2k^0_{\bar{u}} 2k^0_c}{\tilde{k}^0_{\bar{u}} 2\tilde{k}^0_c} \frac{\tilde{k}^0_{\bar{u}} + \tilde{k}^0_c}{k^0_{\bar{u}} + k^0_c}, \tag{3.12}$$

we can make use of the normalization condition for the wave functions

$$\sum_{\mu_{\bar{u}} \mu_c} \int d^3\tilde{k}_{\bar{u}} \Psi^*_{\underline{\alpha}_D \mu_{\bar{u}} \mu_c}(\tilde{\mathbf{k}}) \Psi_{\underline{\alpha}'_D \mu_{\bar{u}} \mu_c}(\tilde{\mathbf{k}}) = \delta_{\underline{\alpha}_D \underline{\alpha}'_D}. \tag{3.13}$$

Comparison of Eq. (3.13) with Eq. (3.10) gives us the scalar product we want to know:

$$\begin{aligned}
&\langle \underline{\mathbf{V}}'; \underline{\mathbf{k}}_D, \underline{\alpha}_D; \underline{\mathbf{k}}_e, \underline{\mu_e} | \mathbf{V}; \mathbf{k}_{\bar{u}}, \mu_{\bar{u}}; \mathbf{k}_c, \mu_c; \mathbf{k}_e, \mu_e \rangle \\
&= (2\pi)^{\frac{15}{2}} \sqrt{\frac{2\underline{k}_D^0 2\underline{k_e}^0}{(\underline{k}_D^0 + \underline{k_e}^0)^3}} \sqrt{\frac{2k_e^0 2k_{\bar{u}c}^0}{(k_e^0 + k_{\bar{u}c}^0)^3}} \sqrt{\frac{2\tilde{k}_{\bar{u}}^0 2\tilde{k}_c^0}{2(\tilde{k}_{\bar{u}}^0 + \tilde{k}_c^0)^3}} \\
&\times V^0 \delta^3(\mathbf{V} - \underline{\mathbf{V}}')\delta^3(\mathbf{k}_e - \underline{\mathbf{k}}_e)\delta_{\mu_e \underline{\mu_e}} \Psi_{\underline{\alpha}_D \mu_{\bar{u}} \mu_c}(\tilde{\mathbf{k}}_{\bar{u}}).
\end{aligned} \tag{3.14}$$

The remaining four scalar products in Eq. (3.8) are computed in a straight forward manner using that

$$\begin{aligned}
&(m - \hat{M}_{\bar{u}bWe})^{-1} | \underline{\mathbf{V}}''; \underline{\mathbf{k}}''_{\bar{u}b}, \underline{\alpha}''_{\bar{u}b}; \underline{\mathbf{k}}''_W, \underline{\mu}''_W; \underline{\mathbf{k}}''_e, \mu''_e \rangle \\
&= (m - \underline{k}''_{\bar{u}b}{}^0 - \underline{k}''_W{}^0 - \underline{k_e}''{}^0)^{-1} | \underline{\mathbf{V}}''; \underline{\mathbf{k}}''_{\bar{u}b}, \underline{\alpha}''_{\bar{u}b}; \underline{\mathbf{k}}''_W, \underline{\mu}''_W; \underline{\mathbf{k}}_e, \mu''_e \rangle.
\end{aligned} \tag{3.15}$$

For the W the sum over the W spin orientation runs over the physical values, i.e. $\mu_W = -1, 0, 1$. Following the same procedure as above the scalar products then become:

$$\begin{aligned}
&\langle \mathbf{V}'; \mathbf{k}'_{\bar{u}}, \mu'_{\bar{u}}; \mathbf{k}'_b, \mu'_b; \mathbf{k}'_W, \mu'_W; \mathbf{k}'_e, \mu'_e | \\
&\times (m - \hat{M}_{\bar{u}bWe})^{-1} | \underline{\mathbf{V}}''; \underline{\mathbf{k}}''_{\bar{u}b}, \underline{\alpha}''_{\bar{u}b}; \underline{\mathbf{k}}''_W, \underline{\mu}''_W; \underline{\mathbf{k}}''_e, \mu''_e \rangle \\
&= (m - \underline{k}''_{\bar{u}b}{}^0 - \underline{k}''_W{}^0 - \underline{k_e}''{}^0)^{-1} (2\pi)^{\frac{21}{2}} \sqrt{\frac{2\tilde{k}'_{\bar{u}}{}^0 2\tilde{k}'_b{}^0}{2(\tilde{k}'_{\bar{u}}{}^0 + \tilde{k}'_b{}^0)}} \\
&\times \sqrt{\frac{2\underline{k}''_{\bar{u}b}{}^0 2\underline{k_e}''{}^0 2\underline{k}''_W{}^0}{(\underline{k}''_{\bar{u}b}{}^0 + \underline{k_e}''{}^0 + \underline{k}''_W{}^0)^3}} \sqrt{\frac{2k'_{\bar{u}b}{}^0 2k''_e{}^0 2k''_W{}^0}{(k'_{\bar{u}b}{}^0 + k''_e{}^0 + k''_W{}^0)^3}} \underline{V}''{}^0 \delta^3(\underline{\mathbf{V}}'' - \mathbf{V}') \\
&\times \delta_{\underline{\mu_e}'' \mu'_e} \delta^3(\underline{\mathbf{k}_e}'' - \mathbf{k}'_e) \delta_{\underline{\mu}''_W \mu'_W} \delta^3(\underline{\mathbf{k}}''_W - \mathbf{k}'_W) \Psi_{\underline{\alpha}''_{\bar{u}b} \mu'_{\bar{u}} \mu'_b}(\tilde{\mathbf{k}}'_{\bar{u}}),
\end{aligned} \tag{3.16}$$

$$\begin{aligned}
&\langle \underline{\mathbf{V}}''; \underline{\mathbf{k}}''_{\bar{u}b}, \underline{\alpha}''_{\bar{u}b}; \underline{\mathbf{k}}''_W, \underline{\mu}''_W; \underline{\mathbf{k}}''_e, \mu''_e | \mathbf{V}''; \mathbf{k}''_{\bar{u}}, \mu''_{\bar{u}}; \mathbf{k}''_b, \mu''_b; \mathbf{k}''_W, \mu''_W; \mathbf{k}''_e, \mu''_e \rangle \\
&= (2\pi)^{\frac{21}{2}} \sqrt{\frac{2\underline{k}''_{\bar{u}b}{}^0 2\underline{k_e}''{}^0 2\underline{k}''_W{}^0}{(\underline{k}''_{\bar{u}b}{}^0 + \underline{k_e}''{}^0 + \underline{k}''_W{}^0)^3}} \sqrt{\frac{2k''_{\bar{u}b}{}^0 2k''_e{}^0 2k''_W{}^0}{(k''_{\bar{u}b}{}^0 + k''_e{}^0 + k''_W{}^0)^3}} \\
&\times \sqrt{\frac{2\tilde{k}''_{\bar{u}}{}^0 2\tilde{k}''_b{}^0}{2(\tilde{k}''_{\bar{u}}{}^0 + \tilde{k}''_b{}^0)}} \underline{V}''{}^0 \delta^3(\underline{\mathbf{V}}'' - \mathbf{V}'') \delta_{\underline{\mu_e}'' \mu''_e} \delta^3(\underline{\mathbf{k}_e}'' - \mathbf{k}''_e) \\
&\times \delta_{\underline{\mu}''_W \mu''_W} \delta^3(\underline{\mathbf{k}}''_W - \mathbf{k}''_W) \Psi_{\underline{\alpha}''_{\bar{u}b} \mu''_{\bar{u}} \mu''_b}(\tilde{\mathbf{k}}''_{\bar{u}}),
\end{aligned} \tag{3.17}$$

$$\begin{aligned}
&\langle \mathbf{V}'''; \mathbf{k}'''_{\bar{u}}, \mu'''_{\bar{u}}; \mathbf{k}'''_{b}, \mu'''_{b}; \mathbf{k}'''_{\nu_e}, \mu'''_{\nu_e} | \underline{\mathbf{V}}; \underline{\mathbf{k}}_B, \underline{\alpha}_B; \underline{\mathbf{k}}_{\nu_e}, \underline{\mu}_{\nu_e} \rangle \\
&= (2\pi)^{\frac{15}{2}} \sqrt{\frac{2\underline{k}^0_B 2\underline{k}^0_{\nu_e}}{(\underline{k}^0_B + \underline{k}^0_{\nu_e})^3}} \sqrt{\frac{2k^0_{\nu_e} 2k'''^{\,0}_{\bar{u}b}}{(k^0_{\nu_e} + k'''^{\,0}_{\bar{u}b})^3}} \sqrt{\frac{2\tilde{k}'''^{\,0}_{\bar{u}} 2\tilde{k}'''^{\,0}_{b}}{2(\tilde{k}'''^{\,0}_{\bar{u}} + \tilde{k}'''^{\,0}_{b})}} \\
&\times \underline{V}^0 \delta^3(\underline{\mathbf{V}} - \mathbf{V}''') \delta^3(\underline{\mathbf{k}}_{\nu_e} - \mathbf{k}'''_{\nu_e}) \delta_{\underline{\mu}_{\nu_e} \mu'''_{\nu_e}} \Psi_{\underline{\alpha}_B \mu'''_{\bar{u}} \mu'''_{b}}(\tilde{\mathbf{k}}'''_{\bar{u}}).
\end{aligned} \tag{3.18}$$

3.1.2 Vertex-Operator Matrix Elements

We have already mentioned in Sec. 2.3 how vertex-operator matrix elements are constructed from interaction Lagrangian densities . Starting with Eq. (2.50) we show the calculation for the matrix elements occurring in Eq. (3.8).

$$\begin{aligned}
&\langle \mathbf{V}; \mathbf{k}_{\bar{u}}, \mu_{\bar{u}}; \mathbf{k}_c, \mu_c; \mathbf{k}_e, \mu_e | \hat{K}_{\bar{u}bWe \to \bar{u}ce} | \mathbf{V}'; \mathbf{k}'_{\bar{u}}, \mu'_{\bar{u}}; \mathbf{k}'_b, \mu'_b; \mathbf{k}'_W, \mu'_W; \mathbf{k}'_e, \mu'_e \rangle \\
&= \frac{(2\pi)^3}{\sqrt{(M_{\bar{u}ce})^3 (M'_{\bar{u}bWe})^3}} V^0 \delta^3(\mathbf{V} - \mathbf{V}') \\
&\times \langle \mathbf{k}_{\bar{u}}, \mu_{\bar{u}}; \mathbf{k}_c, \mu_c; \mathbf{k}_e, \mu_e | \mathcal{L}^{\mathrm{weak}}_{\mathrm{int}}(0) | \mathbf{k}'_{\bar{u}}, \mu'_{\bar{u}}; \mathbf{k}'_b, \mu'_b; \mathbf{k}'_W, \mu'_W; \mathbf{k}'_e, \mu'_e \rangle.
\end{aligned} \tag{3.19}$$

Inserting the weak interaction density

$$\mathcal{L}^{int}_{weak}(0) = \bar{\Psi}(0) \frac{-\imath e V_{\mathrm{cab}}}{2\sqrt{2}\sin\Theta_W} \gamma^\mu (1 - \gamma^5) \Psi(0) W_\mu(0) \tag{3.20}$$

- with Ψ being the quark-field operator,
- e...positron charge
- V_{cab} ...Cabbibo Matrix-element of the flavors involved in the transition
- $\sin\Theta_W$ ...Weinberg mixing-angle
- W_μ...W-boson field

and using the plain-wave expansions for quark and boson fields

$$\begin{aligned}
\hat{\Psi}(x) &= \frac{1}{(2\pi)^3}\sum_{\sigma=\pm\frac{1}{2}}\int\frac{d^3p}{2p^0}\left(\mathrm{e}^{\imath p\cdot x}v_\sigma(\mathbf{p})\hat{d}^\dagger_\sigma+\mathrm{e}^{-\imath p\cdot x}u_\sigma(\mathbf{p})\hat{c}_\sigma(\mathbf{p}\right)\\
\hat{\bar{\Psi}}(x) &= \frac{1}{(2\pi)^3}\sum_{\sigma=\pm\frac{1}{2}}\int\frac{d^3p}{2p^0}\left(\mathrm{e}^{-\imath p\cdot x}\bar{v}_\sigma(\mathbf{p})\hat{d}_\sigma+\mathrm{e}^{-\imath p\cdot x}\bar{u}_\sigma(\mathbf{p})\hat{c}^\dagger_\sigma(\mathbf{p}\right)\\
\hat{W}^\mu(x) &= \frac{1}{(2\pi)^3}\sum_{\sigma=0,\pm1}\int\frac{d^3p}{2p^0}\left(\mathrm{e}^{\imath p\cdot x}\epsilon^\mu(\mathbf{p},\sigma)\hat{a}^\dagger_\sigma(\mathbf{p})+\mathrm{e}^{-\imath p\cdot x}\epsilon^{*\mu}(\mathbf{p},\sigma)\hat{a}_\sigma(\mathbf{p})\right),
\end{aligned} \tag{3.21}$$

the velocity-state matrix element of the interaction density becomes

$$\begin{aligned}
&\frac{1}{(2\pi)^9}\frac{-\imath eV_{\mathrm{cab}}}{2\sqrt{2}\sin\Theta_W}\sum_{\sigma,\sigma',\sigma''}\int\frac{d^3p}{2p^0}\frac{d^3p'}{2p'^{\,0}}\frac{d^3p''}{2p''^{\,0}}\langle\mathbf{V};\mathbf{k}_{\bar{u}},\mu_{\bar{u}};\mathbf{k}_c,\mu_c;\mathbf{k}_e,\mu_e|\\
&\times\left(\bar{v}_\sigma(\mathbf{p})\hat{d}_\sigma+\bar{u}_\sigma(\mathbf{p})\hat{c}^\dagger_\sigma(\mathbf{p})\right)\gamma^\mu(1-\gamma^5)\left(v_{\sigma'}(\mathbf{p}')\hat{d}^\dagger_{\sigma'}(\mathbf{p}')+u_{\sigma'}(\mathbf{p}')\hat{c}_{\sigma'}(\mathbf{p}')\right)\\
&\times\left(\epsilon^\mu(\mathbf{p}'',\sigma'')\hat{a}^\dagger_{\sigma''}(\mathbf{p}'')+\epsilon^{*\ \mu}(\mathbf{p}'',\sigma'')\hat{a}_{\sigma''}(\mathbf{p}'')\right)|\\
&\times\mathbf{V}';\mathbf{k}'_{\bar{u}},\mu'_{\bar{u}};\mathbf{k}'_b,\mu'_b;\mathbf{k}'_W,\mu'_W;\mathbf{k}'_e,\mu'_e\rangle.
\end{aligned} \tag{3.22}$$

Now we collect only those terms which correspond to the transition under investigation, namely $b+W\to c$. All other terms lead to vanishing matrix elements, the only contributing term is

$$\begin{aligned}
&\langle\mathbf{V};\mathbf{k}_{\bar{u}},\mu_{\bar{u}};\mathbf{k}_c,\mu_c;\mathbf{k}_e,\mu_e|\bar{u}_\sigma(\mathbf{p})\hat{c}^\dagger_\sigma(\mathbf{p})\gamma^\mu(1-\gamma^5)u_{\sigma'}(\mathbf{p}')\hat{c}_{\sigma'}(\mathbf{p}')\\
&\times\epsilon^{*\ \mu}(\mathbf{p}'',\sigma'')\hat{a}_{\sigma''}(\mathbf{p}'')|\mathbf{V}';\mathbf{k}'_{\bar{u}},\mu'_{\bar{u}};\mathbf{k}'_b,\mu'_b;\mathbf{k}'_W,\mu'_W;\mathbf{k}'_e,\mu'_e\rangle.
\end{aligned} \tag{3.23}$$

The velocity states can be expressed by creation operators acting on the vacuum.

$$|\vec{k}_1,\mu_1;\vec{k}_2,\mu_2;\ldots;\vec{k}_n,\mu_n\rangle=\hat{c}^\dagger_{\mu_1}(\vec{k}_1)\ldots\hat{c}^\dagger_{\mu_i}(\vec{k}_i)\hat{d}^\dagger_{\mu_{i+1}}(\vec{k}_{i+1})\ldots\hat{d}^\dagger_{\mu_n}(\vec{k}_n)|0\rangle, \tag{3.24}$$

with

$$\begin{aligned}
&\hat{c}^\dagger_{\mu_1}(\vec{k}_1)\ldots\hat{c}^\dagger_{\mu_i}(\vec{k}_i)\ldots\text{quark creation operators and}\\
&\hat{d}^\dagger_{\mu_{i+1}}(\vec{k}_{d+1})\ldots\hat{d}^\dagger_{\mu_n}(\vec{k}_n)\ldots\text{antiquark creation operators.}
\end{aligned} \tag{3.25}$$

Concentrating on the creation and annihilation operators in Eq.(3.23) and expressing the velocity states by means of Eq.(3.24) we get

$$
\begin{aligned}
&\langle \mathbf{k}_{\bar u}, \mu_{\bar u}; \mathbf{k}_c, \mu_c; \mathbf{k}_e, \mu_e | \hat c_\sigma(\mathbf{p}) \hat c^\dagger_{\sigma'}(\mathbf{p}') \hat a_{\sigma''}(\mathbf{p}'') | \mathbf{k}'_{\bar u}, \mu'_{\bar u}; \mathbf{k}'_b, \mu'_b; \mathbf{k}'_W, \mu'_W; \mathbf{k}'_e, \mu'_e \rangle \\
&= \langle 0 | \hat d_{\mu_{\bar u}} \hat c_{\mu_c} \hat c_{\mu_e} \hat c^\dagger_\sigma \hat c_{\sigma'} \hat a_{\sigma''} \hat d^\dagger_{\mu'_{\bar u}} \hat c^\dagger_{\mu'_b} \hat c^\dagger_{\mu'_e} \hat a^\dagger_{\mu'_W} | 0 \rangle \\
&= \langle 0 | (\{\hat d_{\mu_{\bar u}}, \hat d^\dagger_{\mu'_{\bar u}}\} - \hat d^\dagger_{\mu'_{\bar u}} \hat d_{\mu_{\bar u}})(\{\hat c_{\mu_c}, \hat c^\dagger_\sigma\} - \hat c^\dagger_\sigma \hat c_{\mu_c})(\{\hat c_{\mu_e}, \hat c^\dagger_{\mu'_e}\} - \hat c^\dagger_{\mu'_e} \hat c_{\mu_e}) \\
&\times (\{\hat c_{\sigma'}, \hat c^\dagger_{\mu'_b}\} - \hat c^\dagger_{\mu'_b} \hat c_{\sigma'})([\hat a_{\sigma''}, \hat a^\dagger_{\mu'_W}] - \hat a^\dagger_{\mu'_W} \hat a_{\sigma''}) | 0 \rangle .
\end{aligned}
\tag{3.26}
$$

Because all creation operators are acting on the bra and all annihilation operators are acting on the ket, only the product of (anti)commutators gives a non vanishing contribution which can be evaluated by using the (anti)commutation relations

$$
\begin{aligned}
\left\{ \hat c_\sigma(\mathbf{p}), \hat c^\dagger_{\sigma'}(\mathbf{p}') \right\} &= \left\{ \hat d_\sigma(\mathbf{p}), \hat d^\dagger_{\sigma'}(\mathbf{p}') \right\} \\
&= (2\pi)^3 2p^0 \delta^3(\mathbf{p} - \mathbf{p}') \delta_{\sigma\sigma'}, \\
\left[\hat a_\sigma(\mathbf{p}), \hat a^\dagger_{\sigma'}(\mathbf{p}') \right] &= \delta_{\sigma\sigma'} (2\pi)^3 2p^0 \delta^3(\mathbf{p} - \mathbf{p}').
\end{aligned}
\tag{3.27}
$$

After evaluating the summations and integrations by using the appropriate Dirac- and Kronecker-deltas, the interaction-density matrix element (3.22) becomes

$$
\begin{aligned}
&\langle \mathbf{V}; \mathbf{k}_{\bar u}, \mu_{\bar u}; \mathbf{k}_c, \mu_c; \mathbf{k}_e, \mu_e | \hat K_{\bar u b W e \to \bar u c e} | \mathbf{V}'; \mathbf{k}'_{\bar u}, \mu'_{\bar u}; \mathbf{k}'_b, \mu'_b; \mathbf{k}'_W, \mu'_W; \mathbf{k}'_e, \mu'_e \rangle \\
&= \frac{(2\pi)^9}{\sqrt{(M_{\bar u c e})^3 (M'_{\bar u b W e})^3}} V^0 \delta^3(\mathbf{V} - \mathbf{V}') 2k^0_{\bar u} \delta^3(\mathbf{k}_{\bar u} - \mathbf{k}'_{\bar u}) \delta_{\mu_{\bar u}\mu'_{\bar u}} 2k^0_e \delta^3(\mathbf{k}_e - \mathbf{k}'_e) \delta_{\mu_e \mu'_e} \\
&\times \frac{-\imath e V_{\mathrm{cab}}}{\sqrt{2}\sin\Theta_W} \bar u_{\mu_c}(\mathbf{k}_c) \gamma^\mu \frac{(1-\gamma^5)}{2} u_{\mu'_b}(\mathbf{k}'_b) \epsilon^{*\mu}(\vec k'_W, \mu'_W).
\end{aligned}
\tag{3.28}
$$

In the same manner the second vertex-operator matrix element occurring in Eq. (3.8) is obtained:

$$
\begin{aligned}
&\langle \mathbf{V}''; \mathbf{k}''_{\bar{u}}, \mu''_{\bar{u}}; \mathbf{k}''_b, \mu''_b; \mathbf{k}''_W, \mu''_W; \mathbf{k}''_e, \mu''_e | \hat{K}^\dagger_{\bar{u}bWe\to\bar{u}b\nu_e} | \mathbf{V}'''; \mathbf{k}'''_{\bar{u}}, \mu'''_{\bar{u}}; \mathbf{k}'''_b, \mu'''_b; \mathbf{k}'''_{\nu_e}, \mu'''_{\nu_e} \rangle \\
&= \frac{(2\pi)^9}{\sqrt{(M''_{\bar{u}bWe})^3 (M_{\bar{u}b\nu_e})^3}} V''_0 \delta^3(\mathbf{V}'' - \mathbf{V}''') 2k''^{\,0}_{\bar{u}} \delta^3(\mathbf{k}''_{\bar{u}} - \mathbf{k}'''_{\bar{u}}) \delta_{\mu''_{\bar{u}}\mu'''_{\bar{u}}} 2k''^{\,0}_b \\
&\times \delta^3(\mathbf{k}''_b - \mathbf{k}'''_b) \delta_{\mu''_b \mu'''_b} \frac{-\imath e V_{\mathrm{cab}}}{\sqrt{2}\sin\Theta_W} \bar{u}_{\mu''_e}(\mathbf{k}''_e) \gamma^\mu \frac{(1-\gamma^5)}{2} u_{\mu'''_{\nu_e}}(\mathbf{k}'''_{\nu_e}) \epsilon^\mu(\vec{k}''_W, \mu''_W)
\end{aligned}
\tag{3.29}
$$

3.2 Bound-State Current

To extract the bound-state current we have to evaluate the scattering amplitude, Eq.(3.4), by inserting the expressions (3.14), (3.28),(3.16),(3.17),(3.29) and (3.18) into Eq.(3.8). We collect all factors 2π, carry out the integrations over the overall three-velocities by means of the appropriate delta-functions and substitute all spin polarizations according to $\sum_\mu \delta_{\mu\mu'} \Rightarrow \mu \to \mu'$. Also the integrations over the lepton momenta, the exchange particle momenta and the constituent momenta $\mathbf{k}'_{\bar{u}}$, $\mathbf{k}''_{\bar{u}}$ and $\mathbf{k}''_b$ can be carried out by means of corresponding δ-functions.

$$\begin{aligned}
\Gamma_1 = & \frac{(2\pi)^3 \underline{V}^0 \delta^3(\underline{\mathbf{V}} - \underline{\mathbf{V}}')}{(m - \underline{k}''^{\,0}_{\bar{u}b} - k''^{\,0}_W - \underline{k}^0_e)} \\
& \times \sum_{\mu'_{\bar{u}}\mu'_b\mu_c} \sum_{\underline{\mu}''_{\bar{u}b}\mu''_{\bar{u}}\mu''_b} \int\int d^3k_{\bar{u}} d^3k''_{\bar{u}} \frac{(k^0_{\bar{u}} + k^0_c + \underline{k}^0_e)^3}{2k^0_c} \\
& \times \sum_{\mu'_W} \frac{(k^0_{\bar{u}} + k''^{\,0}_W + \underline{k}^0_e + k'^{\,0}_b)}{2k''^{\,0}_W 2\underline{k}^0_e 2k^0_{\bar{u}} 2k'^{\,0}_b} \frac{(\underline{k}''^{\,0}_{\bar{u}b} + k''^{\,0}_W + \underline{k}^0_e)^3}{2k''^{\,0}_W 2\underline{k}^0_e 2\underline{k}''^{\,0}_{\bar{u}b}} \\
& \times \sum_{\underline{\mu}''_W} \delta_{\underline{\mu}''_W \mu'_W} \epsilon^{*\,\nu}(\mathbf{k}'_W, \mu'_W) \frac{(k'''^{\,0}_{\bar{u}} + k''^{\,0}_W + \underline{k}^0_e)^3}{2k'''^{\,0}_{\bar{u}} 2k''^{\,0}_W 2\underline{k}^0_e 2k'''^{\,0}_b} \\
& \times \sum_{\mu''_W} \delta_{\underline{\mu}''_W \mu''_W} \epsilon^{\mu}(\mathbf{k}''_W, \mu''_W) \frac{(k'''^{\,0}_{\bar{u}} + k'''^{\,0}_b + \underline{k}^0_{\nu_e})^3}{2\underline{k}^0_{\nu_e}} \\
& \times \sqrt{\frac{2\underline{k}^0_D 2\underline{k}^0_e}{(\underline{k}^0_D + \underline{k}^0_e)^3}} \frac{\sqrt{2\underline{k}^0_e 2(k^0_{\bar{u}} + k^0_c)}}{(\underline{k}^0_e + k^0_{\bar{u}} + k^0_c)^3} \sqrt{\frac{2\tilde{k}^0_{\bar{u}} 2\tilde{k}^0_c}{2(\tilde{k}^0_{\bar{u}} + \tilde{k}^0_c)}} \Psi^*_{\underline{\alpha}_D \mu_{\bar{u}} \mu_c}(\tilde{\mathbf{k}}_{\bar{u}}) \\
& \times \frac{-\imath e V_{\mathrm{cb}}}{\sqrt{2}\sin\Theta_W} \bar{u}_{\mu_c}(\mathbf{k}_c) \gamma^\nu \frac{1-\gamma^5}{2} u_{\mu'_b}(\mathbf{k}'_{\bar{u}}) \\
& \times \sqrt{\frac{2\tilde{k}'^{\,0}_{\bar{u}} 2\tilde{k}'^{\,0}_b}{2(\tilde{k}'^{\,0}_{\bar{u}} + \tilde{k}'^{\,0}_b)}} \frac{2\underline{k}''^{\,0}_{\bar{u}b} 2\underline{k}^0_e 2k''^{\,0}_W}{(\underline{k}''^{\,0}_{\bar{u}b} + k''^{\,0}_W + \underline{k}^0_e)^3} \\
& \times \frac{\sqrt{2(k'^{\,0}_{\bar{u}} + k'^{\,0}_b) 2\underline{k}^0_e 2k''^{\,0}_W}}{(k'^{\,0}_{\bar{u}} + k'^{\,0}_b + \underline{k}^0_e + k''^{\,0}_W)^3} \Psi_{\underline{\alpha}''_{\mu_{\bar{u}b}} \mu'_{\bar{u}} \mu'_b}(\tilde{\mathbf{k}}'_{\bar{u}}) \\
& \times \frac{-\imath e}{\sqrt{2}\sin\Theta_W} \bar{u}_{\mu_e}(\underline{\mathbf{k}}_e) \gamma^\mu \frac{1-\gamma^5}{2} u_{\mu_{\nu_e}}(\underline{\mathbf{k}}_{\nu_e}) \\
& \times \sqrt{\frac{2\underline{k}^0_B 2\underline{k}^0_{\nu_e}}{(\underline{k}^0_B + \underline{k}^0_{\nu_e})^3}} \frac{\sqrt{2\underline{k}^0_{\nu_e} 2(k'''^{\,0}_{\bar{u}} + k'''^{\,0}_b)}}{(\underline{k}^0_{\nu_e} + k'''^{\,0}_{\bar{u}} + k'''^{\,0}_b)^3} \frac{2\tilde{k}'''^{\,0}_{\bar{u}} 2\tilde{k}'''^{\,0}_b}{2(\tilde{k}'''^{\,0}_{\bar{u}} + \tilde{k}'''^{\,0}_b)} \\
& \times \frac{\sqrt{2(k'''^{\,0}_{\bar{u}} + k'''^{\,0}_b) 2\underline{k}^0_e 2k''^{\,0}_W}}{(k'''^{\,0}_{\bar{u}} + k'''^{\,0}_b + \underline{k}^0_e + k''^{\,0}_W)^3} \Psi_{\underline{\alpha}_B \mu''_{\bar{u}} \mu''_b}(\tilde{\mathbf{k}}'''_{\bar{u}}) \Psi_{\underline{\alpha}_{\bar{u}b} \mu''_{\bar{u}} \mu''_b}(\tilde{\mathbf{k}}'''_{\bar{u}}).
\end{aligned} \tag{3.30}$$

Since $k''_{\bar{u}} = k'''_{\bar{u}}$ and $k''_b = k'''_b$, equivalent identitys also hold for the tilded momenta in the meson center-of-momentum frame. This means that we can substitute $\tilde{k}''_{\bar{u}}$ and $\tilde{k}''_b$ by $\tilde{k}'''_{\bar{u}}$ and $\tilde{k}'''_b$, respectively. As a consequence we can make use of the normalization condition

$$\sum_{\mu''_{\bar{u}}\mu''_b} \int \Psi^*_{\underline{\alpha}''_{\bar{u}b}\mu''_{\bar{u}}\mu''_b}(\tilde{\mathbf{k}}'''_{\bar{u}})\Psi_{\underline{\alpha}_B\mu''_{\bar{u}}\mu''_b}(\tilde{\mathbf{k}}'''_{\bar{u}})d^3\tilde{k}'''_{\bar{u}} = \delta_{\underline{\alpha}''_{\bar{u}b}\underline{\alpha}_B}, \tag{3.31}$$

where we have used the transformed integration measure, Eq.(3.12). By using the same integral transformation for the remaining $\tilde{k}_{\bar{u}}$ together with the completeness relation for the W-boson polarization vectors

$$\sum_{\sigma=0,\pm 1} \epsilon^\mu(\mathbf{k},\sigma)\epsilon^{*\ \nu}(\mathbf{k},\sigma) = -g^{\mu\nu} + \frac{k^\mu k^\nu}{m_W^2}, \tag{3.32}$$

we finally obtain

$$\begin{aligned}
\Gamma_1 \quad = \quad & (2\pi)^3 \underline{V}^0 \delta^3(\underline{\mathbf{V}} - \underline{\mathbf{V}}') \frac{1}{(\underline{k}_D^0 + \underline{k}_e^0)^3 (\underline{k}_B^0 + \underline{k}_{\nu_e}^0)^3} \\
& \times \frac{-e^2 V_{\mathrm{cb}}}{2\sin\Theta_W{}^2} \frac{1}{2} \bar{u}_{\mu_e}(\underline{\mathbf{k}}_e)\gamma^\mu(1-\gamma^5)u_{\mu_{\nu_e}}(\underline{\mathbf{k}}_{\nu_e}) \\
& \times \frac{(-g^{\mu\nu} + \frac{k_W^\mu k_W^\nu}{m_W^2})}{2k''^{\,0}_W(m - \underline{k}''^{\,0}_{\bar{u}b} - k''^{\,0}_W - \underline{k}_e^0)} \frac{1}{2} 2\sqrt{\underline{k}_D^0 \underline{k}_B^0} \int \frac{d^3\tilde{k}_{\bar{u}}}{2k'^{\,0}_b} \\
& \times \sqrt{\frac{k'^{\,0}_{\bar{u}} + k'^{\,0}_b}{k^0_{\bar{u}} + k^0_c}} \sqrt{\frac{\tilde{k}^0_{\bar{u}} + \tilde{k}^0_c}{\tilde{k}'^{\,0}_{\bar{u}} + \tilde{k}'^{\,0}_b}} \sqrt{\frac{\tilde{k}'^{\,0}_{\bar{u}}\tilde{k}'^{\,0}_b}{\tilde{k}^0_{\bar{u}}\tilde{k}^0_c}} \\
& \times \sum_{\mu'_{\bar{u}}\mu'_b\mu_c} \bar{u}_{\mu_c}(\mathbf{k}_c)\gamma^\nu(1-\gamma^5)u_{\mu'_b}(\mathbf{k}'_b)\Psi_{\underline{\alpha}_D\mu'_{\bar{u}}\mu_c}(\tilde{\mathbf{k}}_{\bar{u}})\Psi_{\underline{\alpha}_B\mu'_{\bar{u}}\mu'_b}(\tilde{\mathbf{k}}'_{\bar{u}}).
\end{aligned} \tag{3.33}$$

In a straight forward manner the second time-ordered contribution to the scattering amplitude, Eq.(3.4), is obtained. Both time orderings differ only in the propagator, but because all particles are on their mass-shell both terms sum up to the covariant W-propagator [5]:

$$\begin{aligned}
& \frac{1}{2k_W^0}\left(\frac{1}{m-k_B^0-k_W^0-k_e^0)}+\frac{1}{m-k_D^0-k_W^0-k_{\nu_e}^0}\right) \\
= \;& \frac{1}{2k_W^0}\left(\frac{1}{(k_{\nu_e}^0-k_e^0)-k_W^0}+\frac{1}{-(k_{\nu_e}^0-k_e^0)-k_W^0}\right) \\
= \;& \frac{1}{(k_{\nu_e}^0-k_e^0)^2-{k_W^0}^2} \\
= \;& \frac{1}{q^2-m_W^2}.
\end{aligned} \tag{3.34}$$

Comparing our result with the scattering amplitude one expects from leading order perturbative quantum field theory, we can identify the hadronic current for the $B-D$ transition in a unique way. So finally we are left with the 1-W-exchange scattering amplitude

$$\begin{aligned}
& \langle \underline{\mathbf{V}}'; \underline{\mathbf{k}}_D, \underline{\alpha}_D; \underline{\mathbf{k}}_e, \underline{\mu}_e | \hat{V}_{\text{opt}}^{\bar{u}b\nu_e \to \bar{u}ce}(m) | \underline{\mathbf{V}}; \underline{\mathbf{k}}_B, \underline{\alpha}_B; \underline{\mathbf{k}}_{\nu_e}, \underline{\mu}_{\nu_e} \rangle \\
= \;& \underline{V}^0 \delta^3(\underline{\mathbf{V}}-\underline{\mathbf{V}}') \frac{(2\pi)^3}{(\underline{k}_D^0+\underline{k}_e^0)^3(\underline{k}_B^0+\underline{k}_{\nu_e}^0)^3} \\
\times \;& \frac{-e^2 V_{\text{cb}}}{2\sin{\Theta_W}^2} \frac{1}{2} \bar{u}_{\mu_e}(\underline{\mathbf{k}}_e)\gamma^\mu(1-\gamma^5)u_{\mu_{\nu_e}}(\underline{\mathbf{k}}_{\nu_e}) \\
\times \;& \frac{(-g^{\mu\nu}+\frac{k_W^\mu k_W^\nu}{m_W^2})}{q^2-m_W^2} \frac{1}{2} J^\nu_{B\to D}(\underline{\mathbf{k}}_B, \underline{\alpha_B}; \underline{\mathbf{k}}_D, \underline{\alpha}_D)
\end{aligned} \tag{3.35}$$

and the bound state current

$$\begin{aligned}
& J^\nu_{B\to D}(\underline{\mathbf{k}}_B, \underline{\alpha_B}; \underline{\mathbf{k}}_D, \underline{\alpha}_D) = \\
& 2\sqrt{\underline{k}_D^0 \underline{k}_B^0} \int \frac{d^3\tilde{k}_{\bar{u}}}{2{k'_b}^0} \sqrt{\frac{{k'_{\bar{u}}}^0+{k'_b}^0}{k_{\bar{u}}^0+k_c^0}} \sqrt{\frac{\tilde{k}_{\bar{u}}^0+\tilde{k}_c^0}{{\tilde{k}'_{\bar{u}}}{}^0+{\tilde{k}'_b}{}^0}} \sqrt{\frac{{\tilde{k}'_{\bar{u}}}{}^0 {\tilde{k}'_b}{}^0}{\tilde{k}_{\bar{u}}^0 \tilde{k}_c^0}} \\
& \times \sum_{\mu'_{\bar{u}}\mu'_b\mu_c} \bar{u}_{\mu_c}(\mathbf{k}_c)\gamma^\nu(1-\gamma^5)u_{\mu'_b}(\mathbf{k}'_b)\Psi^*_{\underline{\alpha}_D\mu'_{\bar{u}}\mu_c}(\tilde{\mathbf{k}}_{\bar{u}})\Psi_{\underline{\alpha}_B\mu'_{\bar{u}}\mu'_b}(\tilde{\mathbf{k}}'_{\bar{u}}).
\end{aligned} \tag{3.36}$$

3.2.1 Pseudoscalar Current

Now we will have a closer look on the overlap of incoming and outgoing meson wave functions in the bound state current, Eq.(3.36). In Sec. 2.2.3 we

[5] q refers to the four-momentum transfer during the scattering process and is defined as $q^\mu = (p_B - p_D)^\mu = (p_e - p_{\nu_e})^\mu$.

have already given a general definition of the two-body bound state wave function, Eq.(2.39), where the angular and radial part, of course, depend on the specific potential used to model instantaneous confinement. Using Eq.(2.39), the overlap of meson wave functions together with the summations over the constituent spin polarizations can be expressed as:

$$
\begin{aligned}
&\sum_{\mu_c\mu'_{\bar{u}}\mu'_b} \Psi^*_{\underline{\alpha}_D\mu'_{\bar{u}}\mu_c}(\tilde{\mathbf{k}}_{\bar{u}})\Psi_{\underline{\alpha}_B\mu'_{\bar{u}}\mu'_b}(\tilde{\mathbf{k}}'_{\bar{u}}) \\
&= \sum_{\mu_c\mu'_{\bar{u}}\mu'_b}\ \sum_{ls\mu_l\mu_s\tilde{\mu}_{\bar{u}}\tilde{\mu}_c}\ \sum_{l's'\mu'_l\mu'_s\tilde{\mu}'_{\bar{u}}\tilde{\mu}'_b} \\
&\times Y^*_{l\mu_l}(\tilde{\mathbf{k}}_{\bar{u}})C^{s\mu_s\ *}_{j_{\bar{u}}\tilde{\mu}_{\bar{u}}j_c\tilde{\mu}_c}C^{j\mu_j\ *}_{l\mu_l s\mu_s}u^{j\ *}_{nls}(\tilde{k}_{\bar{u}}) \\
&\times Y_{l'\mu'_l}(\tilde{\mathbf{k}}'_{\bar{u}})C^{s'\mu'_s}_{j'_{\bar{u}}\tilde{\mu}'_{\bar{u}}j'_b\tilde{\mu}'_b}C^{j'\mu'_j}_{l'\mu'_l s'\mu'_s}u^{j'}_{n'l's'}(\tilde{k}'_{\bar{u}}) \\
&\times D^{j_{\bar{u}}\ *}_{\mu'_{\bar{u}}\tilde{\mu}_{\bar{u}}}[\underline{R}_W(\tilde{\omega}_{\bar{u}}, B_c(\boldsymbol{\omega}_{\bar{u}c}))]D^{j_c\ *}_{\mu_c\tilde{\mu}_c}[\underline{R}_W(\tilde{\omega}_c, B_c(\boldsymbol{\omega}_{\bar{u}c}))] \\
&\times D^{j'_{\bar{u}}}_{\mu'_{\bar{u}}\tilde{\mu}'_{\bar{u}}}[\underline{R}_W(\tilde{\omega}'_{\bar{u}}, B_c(\boldsymbol{\omega}'_{\bar{u}b}))]D^{j'_b}_{\mu'_b\tilde{\mu}'_b}[\underline{R}_W(\tilde{\omega}'_b, B_c(\boldsymbol{\omega}'_{\bar{u}b}))].
\end{aligned}
\tag{3.37}
$$

Here we have used the abbreviations for the four-velocities

$$
\begin{aligned}
\omega_{12} &= \frac{k_{12}}{m_{12}} = \frac{k_1 + k_2}{\sqrt{k^\mu_{12}k_{12\ \mu}}}, \\
\tilde{\omega}_i &= \frac{\tilde{k}_i}{m_i}, \\
\tilde{k}_i &= B_c^{-1}(\boldsymbol{\omega}_{12})k_i.
\end{aligned}
$$

If we consider the meson wave function to be pure s-wave, the angular part as well as the Clebsh-Gordan coefficients simplify to

$$
Y^*_{00} = Y_{00} = \frac{1}{\sqrt{4\pi}},\ C^{j\mu_j}_{00s\mu_s} = \delta_{sj}\delta_{\mu_s\mu_j},\ C^{j'\mu'_j}_{00s'\mu'_s} = \delta_{s'j'}\delta_{\mu'_s\mu'_j}. \tag{3.38}
$$

For the case of pseudoscalar to pseudoscalar transitions, on which we will restrict our treatment, the remaining Clebsh Gordan coefficients give

$$
C^{00}_{\frac{1}{2}\tilde{\mu}_{\bar{u}}\frac{1}{2}\tilde{\mu}_c} = \frac{(-1)^{1-\tilde{\mu}_c}}{\sqrt{2}}\delta_{\tilde{\mu}_c-\tilde{\mu}_{\bar{u}}},\ C^{00}_{\frac{1}{2}\tilde{\mu}'_{\bar{u}}\frac{1}{2}\tilde{\mu}'_b} = \frac{(-1)^{1-\tilde{\mu}'_b}}{\sqrt{2}}\delta_{\tilde{\mu}'_b-\tilde{\mu}'_{\bar{u}}}.
$$

Therefore Eq.(3.37) becomes

$$
\begin{aligned}
&\sum_{\mu_c\mu'_{\bar u}\mu'_b} \Psi^*_{\underline{\alpha}_D\mu'_{\bar u}\mu_c}(\tilde{\mathbf{k}}_{\bar u})\Psi_{\underline{\alpha}_B\mu'_{\bar u}\mu'_b}(\tilde{\mathbf{k}}'_{\bar u})\\
&= \sum_{\mu_c\mu'_{\bar u}\mu'_b}\sum_{\tilde\mu_c\tilde\mu_{\bar u}} \frac{1}{4\pi} u^{0\,*}_{n00}(\tilde k_{\bar u}) u^0_{n'00}(\tilde k'_{\bar u}) \frac{(-1)^{1-\tilde\mu_c-\tilde\mu'_b}}{2}\\
&\times D^{\frac{1}{2}\,*}_{\mu'_{\bar u}-\tilde\mu_c}[\underline{R}_W(\tilde\omega_{\bar u}, B_c(\boldsymbol{\omega}_{\bar u c}))] D^{\frac{1}{2}\,*}_{\mu_c\tilde\mu_c}[\underline{R}_W(\tilde\omega_c, B_c(\boldsymbol{\omega}_{\bar u c}))]\\
&\times D^{\frac{1}{2}}_{\mu'_{\bar u}-\tilde\mu'_b}[\underline{R}_W(\tilde\omega'_{\bar u}, B_c(\boldsymbol{\omega}'_{\bar u b}))] D^{\frac{1}{2}}_{\mu'_b\tilde\mu'_b}[\underline{R}_W(\tilde\omega'_b, B_c(\boldsymbol{\omega}'_{\bar u b}))]\\
&= \frac{1}{8\pi}\sum_{\mu_c\mu'_b} u^*_n(\tilde k_{\bar u}) u_{n'}(\tilde k'_{\bar u}) D^{\frac{1}{2}}_{\mu'_b\mu_c}[\underline{R}_W(\tilde\omega'_b, B_c(\boldsymbol{\omega}'_{\bar u b}))\times\\
&\times\ \underline{R}^{-1}_W(\tilde\omega'_{\bar u}, B_c(\boldsymbol{\omega}'_{\bar u b}))\underline{R}_W(\tilde\omega_{\bar u}, B_c(\boldsymbol{\omega}_{\bar u c}))\underline{R}^{-1}_W(\tilde\omega_c, B_c(\boldsymbol{\omega}_{\bar u c}))]. \qquad (3.39)
\end{aligned}
$$

Inserting this into Eq.(3.36) for the bound state current, we obtain

$$
\begin{aligned}
&J^\nu_{B\to D}(\underline{\mathbf{k}}_B, \underline{\alpha_B}; \underline{\mathbf{k}}_D, \underline{\alpha}_D) =\\
&\frac{\sqrt{\underline{k}^0_D\underline{k}^0_B}}{4\pi}\int \frac{d^3\tilde k_{\bar u}}{2k'^{\,0}_b}\sqrt{\frac{k'^{\,0}_{\bar u}+k'^{\,0}_b}{k^0_{\bar u}+k^0_c}}\sqrt{\frac{\tilde k^0_{\bar u}+\tilde k^0_c}{\tilde k'^{\,0}_{\bar u}+\tilde k'^{\,0}_b}}\sqrt{\frac{\tilde k'^{\,0}_{\bar u}\tilde k'^{\,0}_b}{\tilde k^0_{\bar u}\tilde k^0_c}}\\
&\times\sum_{\mu'_b\mu_c}\bar u_{\mu_c}(\mathbf{k}_c)\gamma^\nu(1-\gamma^5)u_{\mu'_b}(\mathbf{k}'_b)u^*_n(\tilde k_{\bar u})u_{n'}(\tilde k'_{\bar u})\\
&\times D^{\frac{1}{2}}_{\mu'_b\mu_c}[\underline{R}_W(\tilde\omega'_b, B_c(\boldsymbol{\omega}'_{\bar u b}))\ \underline{R}^{-1}_W(\tilde\omega'_{\bar u}, B_c(\boldsymbol{\omega}'_{\bar u b}))\times\\
&\qquad\times\underline{R}_W(\tilde\omega_{\bar u}, B_c(\boldsymbol{\omega}_{\bar u c}))\underline{R}^{-1}_W(\tilde\omega_c, B_c(\boldsymbol{\omega}_{\bar u c}))]. \qquad (3.40)
\end{aligned}
$$

Chapter 4

Spacelike Form Factors

Having now an expression for the bound-state current in terms of constituent currents and bound-state wave functions at hand, we can calculate the current numerically and obtain weak form factors as they could, in principle, be measured in different meson-neutrino scattering processes like $B^- + \nu_e \to D^0 + e^-$, $B^- + \nu_e \to \pi^0 + e^-$ and $D^- + \nu_e \to \pi^0 + e^-$.

4.1 Covariant Decomposition

The general covariant structure of a weak pseudoscalar current is determined by two covariants which can be built with $p_{\alpha'}$ and p_α, the four-momenta of the incoming and outgoing mesons. Each covariant is multiplied with a Lorentz scalar that can only depend on the momentum transfer squared:

$$J^\mu(p_\alpha, p_{\alpha'}) = (p_{\alpha'} + p_\alpha)^\mu F^+(q^2) + (p_{\alpha'} - p_\alpha)^\mu F^-(q^2). \tag{4.1}$$

An equivalent decomposition for such a current is given by [WSB85]

$$J^\mu(p_\alpha, p_{\alpha'}) = \left((p_{\alpha'} + p_\alpha)^\mu - \frac{m_{\alpha'}^2 - m_\alpha^2}{q^2} q^\mu \right) F_1(q^2) + \frac{m_{\alpha'}^2 - m_\alpha^2}{q^2} q^\mu F_0(q^2). \tag{4.2}$$

The four-momentum transfer is defined as $q = p_{\alpha'} - p_\alpha$[1] with $q^2 = q^\mu q_\mu$. By comparing both decompositions it follows immediately that

$$\begin{aligned} F_1(q^2) &= F^+(q^2). \\ F_0(q^2) &= F^+(q^2) + \frac{q^2}{m_{\alpha'}^2 - m_\alpha^2} F^-(q^2). \end{aligned} \tag{4.3}$$

[1]Primed variables refer to the incoming- and unprimed to the outgoing meson.

We have already mentioned in Sec. 2.2.2 that the Bakamjian-Thomas construction spoils cluster separability. As soon as a spectator is present in a Bakamjian-Thomas type mass operator, it influences the interaction via the overall velocity-conserving delta function. This delta function is necessary due to the splitting of the four-momentum operator into the product of an interacting mass operator and a free four-velocity operator (see Eq. (2.32)). This argument holds for both types of interactions used in this work, instantaneous confinement interactions as well as vertex interactions (recall Eqs. (2.40),(2.41) and (2.50)). As a consequence it is conceivable that the current also depends on a covariant made up by the spectator's momenta. This would give rise to an additional unphysical form factor. In contrast to electromagnetic form factors of heavy-light mesons calculated within this framework (cf. [GR11]), where this happens, this is not the case for weak meson transition form factors. However, the violation of cluster separability enters our description through a Mandelstam s dependence of the form factors. This means that the form factors in the covariant decomposition of the bound state current, Eq. (4.2), are not functions of the momentum transfer squared alone, but also of the invariant mass squared of the electron-meson system (i.e. Mandelstam s):

$$J^\mu(p_\alpha, p_{\alpha'}) = \left((p_{\alpha'} + p_\alpha)^\mu - \frac{m_{\alpha'}^2 - m_\alpha^2}{q^2} q^\mu\right) F_1(q^2, s) + \frac{m_{\alpha'}^2 - m_\alpha^2}{q^2} q^\mu F_0(q^2, s). \tag{4.4}$$

The s-dependence of the form factors may also be interpreted as a dependence on the frame in which the $\gamma^* M \to M'$ subprocess is considered. It is not for the violation of cluster separability alone, that we experience this frame dependence of the form factors. Also the contributions of non-valence degrees of freedom, in particular Z-graphs, depend on the invariant mass of the system. It is known for front-form dynamics that Z-graphs vanish when one uses the $q^+ = 0$ Drell-Yan-West frame [BCJ03]. This also holds for the infinite momentum frame in instant form. For a more detailed discussion and a good overview on the correspondence between front form dynamics and the infinite momentum frame in instant form, we refer to [JISu13]. Owing to the suppression of Z-graphs, the infinite-momentum frame thus seems to be preferable for the extraction of hadron form factors as long as one works only within a valence-quark picture. For finite particle momenta, on the other hand, non-valence degrees-of-freedom are likely to play a non-negligible role and a pure valence-quark description may miss part of the physics.

4.2 Kinematics

To analyze the s-dependence addressed above, we calculate the current, Eq. (3.40), numerically using two particular kinematic settings. These are the infinite-momentum-frame, where the invariant mass of the system approaches infinity and the Breit frame which corresponds to the minimal invariant mass necessary to obtain a specific momentum transfer $\sqrt{-q^2}$. Before specifying the kinematics, we recall the transformation properties of velocity states under a Lorentz transformation as given by Eq.(2.23):

$$\hat{U}_{12\ldots n}(\underline{\Lambda})|V;\{\mathbf{k}_i,\mu_i\}\rangle = \sum_{\{\mu_i'\}} |\Lambda V;\{\mathbf{R_{W_c}}(\mathbf{V},\mathbf{\Lambda})\mathbf{k_i},\mu_i'\}\rangle \prod_{i=1}^{n} D^{j_i}_{\mu_i',\mu_i}[\underline{R_{W_c}}(V,\Lambda)].$$

They do not transform like a four-vector but rather by a Wigner rotation. As a result also the current, Eq. (3.40), $J^\nu(\underline{\mathbf{k}}_{\alpha'};\underline{\mathbf{k}}_\alpha)$ transforms by a Wigner rotation. To obtain a covariant quantity, one has to boost it to physical momenta $\underline{\mathbf{p}}_{\alpha'}$ and $\underline{\mathbf{p}}_\alpha$. A possibility to avoid this Lorentz boost, but still obtain a covariant current, is to choose a frame in which the physical momenta automatically fulfill the velocity-state constraint $\sum_{i=1}^n \mathbf{k}_i = 0$. Therefore it is very natural to work with center-of-momentum kinematics. We choose the scattering plane to be the (1,3) plane and the three-momentum of the incoming meson to have a non vanishing component in 1-direction only. As a result, the meson and lepton momenta are parametrized as follows:

$$\underline{p}_{\alpha'} = \begin{pmatrix} \sqrt{m_{\alpha'}^2 + p'^{\,2}} \\ p' \\ 0 \\ 0 \end{pmatrix}, \quad p_{\nu_e} = \begin{pmatrix} \sqrt{m_{\nu_e}^2 + p'^{\,2}} \\ -p' \\ 0 \\ 0 \end{pmatrix}$$
$$\underline{p}_{\alpha} = \begin{pmatrix} \sqrt{m_{\alpha}^2 + p^2} \\ p_1 \\ 0 \\ p_3 \end{pmatrix}, \quad p_{e} = \begin{pmatrix} \sqrt{m_{e}^2 + p^2} \\ -p_1 \\ 0 \\ -p_3 \end{pmatrix}. \tag{4.5}$$

Here p' and p are the absolute values of incoming and outgoing three-momenta, respectively. The kinematics is fixed by two variables. The magnitude of the four-momentum transfer squared $(-q^2)$ and Mandelstam s. If we neglect the lepton masses, p and p' can be expressed through s according to

$$\begin{aligned} s = & \quad (E_{\alpha'} + E_{\nu_e})^2 = & (E_\alpha + E_e)^2 \\ = & \quad (\sqrt{m_{\alpha'}^2 + p'^{\,2}} + p')^2 = & (\sqrt{m_\alpha^2 + p^2} + p)^2, \end{aligned} \tag{4.6}$$

which implies

$$p'^{\,2} = \frac{(s - m_{\alpha'}^2)^2}{4s}, \quad p^2 = \frac{(s - m_\alpha^2)^2}{4s}. \tag{4.7}$$

For scattering, we deal with spacelike momentum transfer. This means that $q^2 = q^\mu q_\mu = -Q^2$, where the transfer of four-momentum is defined as

$$q = p_{\alpha'} - p_\alpha = \begin{pmatrix} E_{\alpha'} - E_\alpha \\ p' - p_1 \\ 0 \\ -p_3 \end{pmatrix}. \tag{4.8}$$

Solving Eqs. (4.6) and

$$-Q^2 = (E_{\alpha'} - E_\alpha)^2 - (\boldsymbol{p}_{\alpha'} - \boldsymbol{p}_\alpha)^2 \tag{4.9}$$

yields p_1 and p_3 in terms of Q^2 and s, which completes the momentum parametrization, Eq.(4.5).

4.2.1 Infinite-Momentum Frame

Extracting the form factors in the infinite-momentum frame is equivalent to performing the limit $s \to \infty$. With the momentum parametrization, Eq.(4.5), and infinitely large Mandelstam s the four components of the current, Eq. (4.2), become

$$\begin{aligned} J^0(p_\alpha, p_{\alpha'}) \to F_1\sqrt{s}, \quad & J^1(p_\alpha, p_{\alpha'}) \to F_1\sqrt{s}, \\ J^2(p_\alpha, p_{\alpha'}) \to 0, \quad & J^3(p_\alpha, p_{\alpha'}) \to \frac{F_0(m_{\alpha'}^2 - m_\alpha^2) + F_1(m_{\alpha'}^2 - m_\alpha^2 + Q^2)}{\sqrt{Q^2}}. \end{aligned} \tag{4.10}$$

We choose $J^0(p_\alpha, p_{\alpha'})$ and $J^3(p_\alpha, p_{\alpha'})$ as linear independent components from which we extract the form factors according to

$$F_1 = \frac{J^0(p_\alpha, p_{\alpha'})}{\sqrt{s}}, \quad F_0 = \frac{J^3(p_\alpha, p_{\alpha'})\sqrt{Q^2} + J^0(p_\alpha, p_{\alpha'})(m_{\alpha'}^2 - m_\alpha^2 - Q^2)\sqrt{\frac{1}{s}}}{m_{\alpha'}^2 - m_\alpha^2}. \tag{4.11}$$

4.2.2 Breit Frame

In the Breit frame, in addition to the center-of-momentum kinematics, in- and outgoing particles have opposite directions (backward scattering). For our parametrization, Eq.(4.5), this means a vanishing 3-component in $p_{\alpha'}$ and p_α. This restriction implies a definite value for s depending on the involved masses and Q^2:

$$p_3 = 0 \Rightarrow s = \frac{1}{2}(m_{\alpha'}^2 + m_\alpha^2 + Q^2 + \sqrt{(m_{\alpha'}^2 + m_\alpha^2 + Q^2)^2 - 4m_{\alpha'}^2 m_\alpha^2}. \quad (4.12)$$

This means that s is not fixed, but rather a function of Q^2. This is not so important for spacelike momentum transfers, but plays a role for the analytic continuation of the form factors into the timelike region. We will return to this issue when discussing timelike form factors.

4.3 Results

The aim of this section is not to provide quantitative results for meson transition form factors, since there are no experimental data to compare with, but rather to discuss the frame dependence of our form factor calculation due to the Bakamjian-Thomas approach. To calculate the bound-state current, Eq. (3.36), we use a simple harmonic-oscillator wave function for the meson:

$$u_n(\tilde{k}) = u_0(\tilde{k}) = \frac{2}{\sqrt[4]{\pi} a^{\frac{3}{2}}} \, e^{-\frac{\tilde{k}^2}{2a^2}}. \quad (4.13)$$

The harmonic-oscillator parameter as well as the constituent masses are taken from [CCH97], where they had been fitted to reproduce meson decay constants. For the meson masses we use the Particle Data Group values [PDG12]. All parameters used are collected in Tab. 4.1. In Figs. 4.1-4.2 we show our results for the form factors F_1 and F_0, calculated in the infinite-momentum frame and the Breit frame, respectively, as functions of Q^2 for different transitions. The frame dependence is indicated by the shaded areas. Compared to the absolute value of the form factors we find a rather mild frame dependence for all B meson transition form factors, whereas the D meson transition form factors (Figs. 4.3-4.4) depend much more on whether we use the infinite-momentum frame (IF) or the Breit frame (BF). We will argue in Sec. 5 that the difference between infinite-momentum frame and Breit-frame results can be (partly) attributed to missing Z-graph contributions in the Breit frame. If these contributions are modeled by meson-pole terms, the smaller frame-dependence of B decays as compared to D-decays may then be traced back to the pole being closer to the physical region of neutrino-meson scattering in case of the D than in case of the B.

Table 4.1: Model parameters

$M_B = 5.2795$ GeV	$m_b = 4.8$ GeV	$a_B = 0.55$
$M_D = 1.869$ GeV	$m_c = 1.6$ GeV	$a_D = 0.46$
$M_\pi = 0.1396$ GeV	$m_{u,d} = 0.25$ GeV	$a_\pi = 0.33$
$M_K = 0.4937$ GeV	$m_s = 0.4$ GeV	$a_K = 0.38$

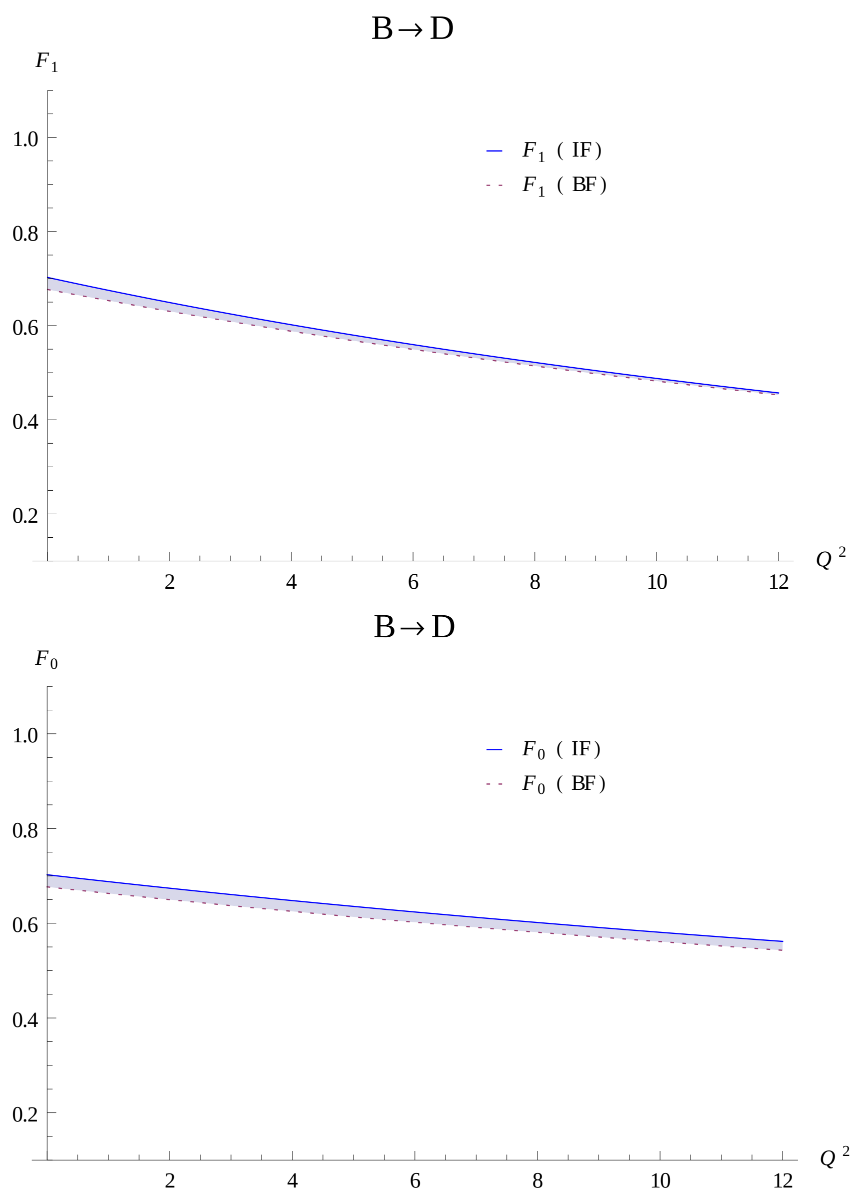

Figure 4.1: Space-like form factors F_1 (top) and F_0 (bottom) for the weak B-D transition calculated in the infinite-momentum-frame (solid line) and the Breit-frame (dashed line). The shaded area indicates the frame dependence.

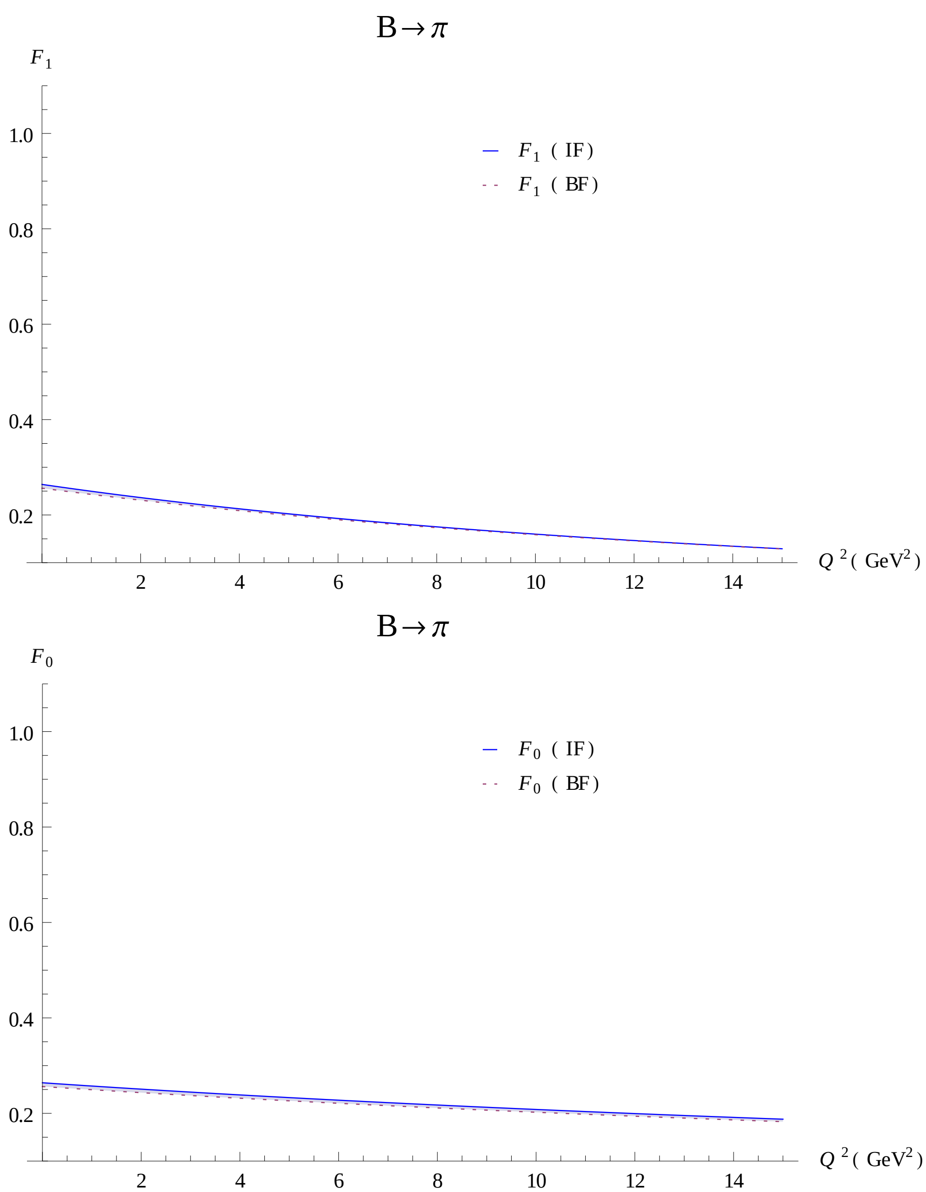

Figure 4.2: Space-like form factors F_1 (top) and F_0 (bottom) for the weak B-π transition calculated in the infinite-momentum-frame (solid line) and the Breit-frame (dashed line). The shaded area indicates the frame dependence.

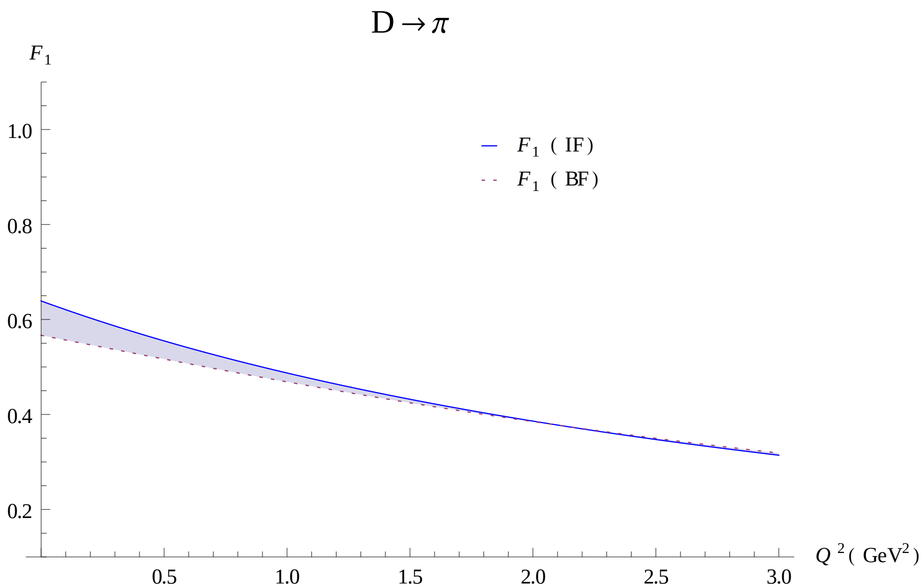

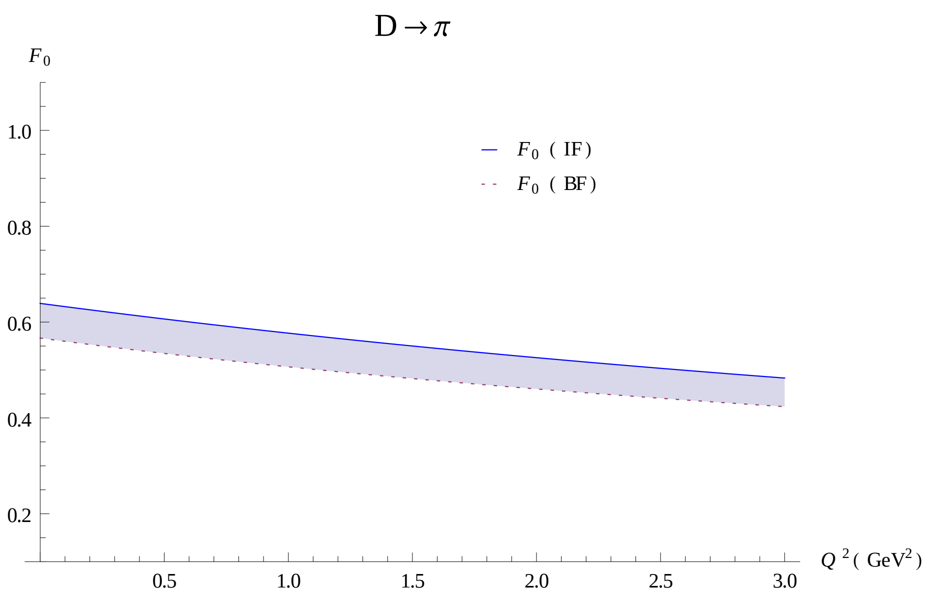

Figure 4.3: Space-like form factors F_1 (top) and F_0 (bottom) for the weak D-π transition calculated in the infinite-momentum-frame (solid line) and the Breit-frame (dashed line). The shaded area indicates the frame dependence.

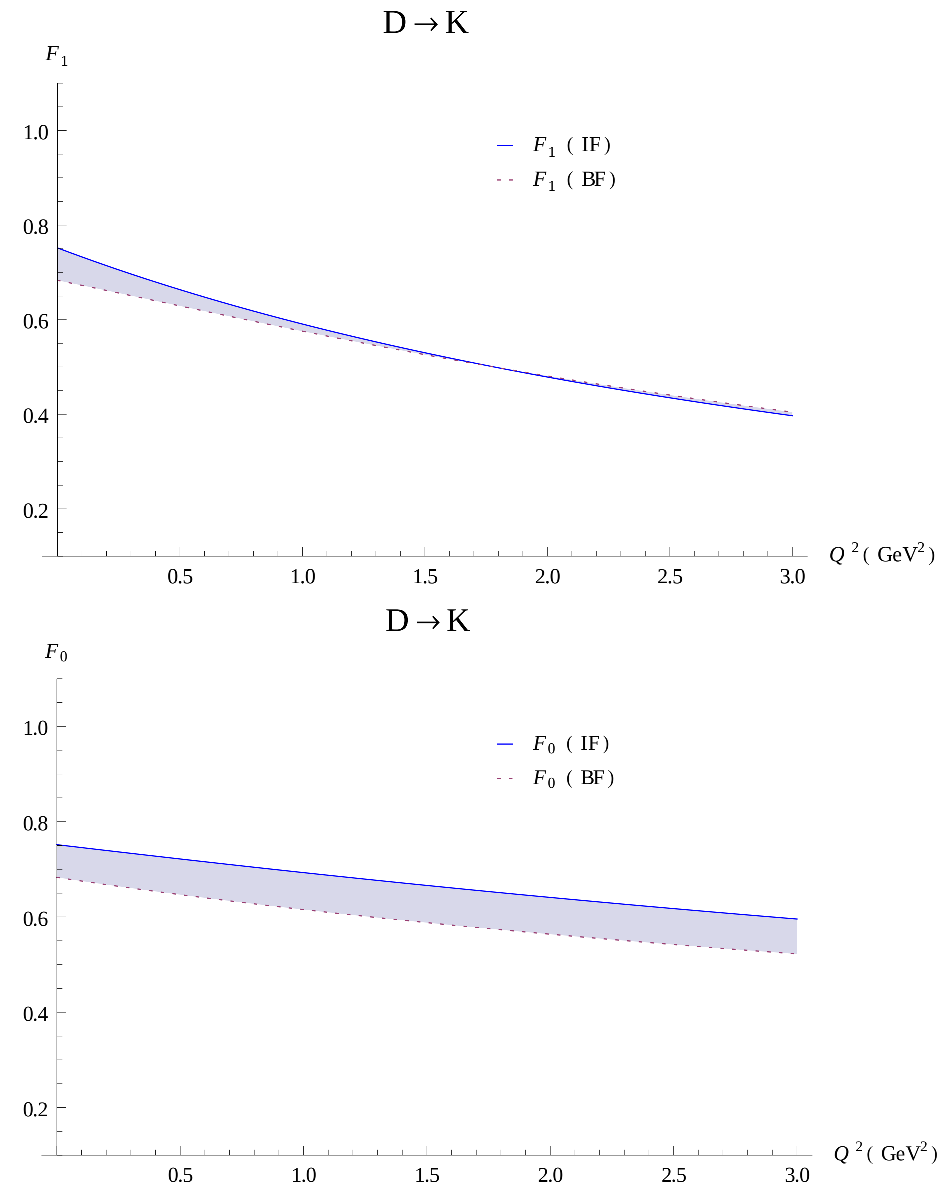

Figure 4.4: Space-like form factors F_1 (top) and F_0 (bottom) for the weak D-K transition calculated in the infinite-momentum-frame (solid line) and the Breit-frame (dashed line). The shaded area indicates the frame dependence.

Chapter 5

Timelike Form Factors

In contrast to scattering processes, where the momentum transfer squared is negative, decay processes are timelike and give rise to positive momentum transfer squared:

- $q^\mu q_\mu < 0 \ldots$ scattering,
- $q^\mu q_\mu \geq 0 \ldots$ decay.

The lepton-meson scattering amplitude is known to be a meromorphic function of the Mandelstam variables s and t. Hence form factors are also expected to be meromorphic functions of $t = q^\mu q_\mu$, the momentum transfer squared. Therefore it is possible to continue them analytically from $q^2 \leq 0$ to $q^2 \geq 0$. In our case and with the momentum parametrization used, this means that we have to substitute $Q \to \imath\, Q$ in Eq. (4.5). This can be done in both, the infinite momentum frame and the Breit frame. Within the front form formalism Z-graphs vanish in a specific kinematic setting, the Drell-Yan-West frame [Si02, MeSi02]. It is also known that Z-graphs vanish in the infinite-momentum frame in instant form [JISu13]. Since the physical reason of the latter observation is the vanishing probability for creating an infinitely fast moving quark-antiquark pair out of the vacuum, we expect Z-graph contributions also to be suppressed in our point form calculations, when we use the infinite-momentum frame. Therefore the major part of this chapter deals with the infinite-momentum kinematics. To strenghen our further line of argumentation, it is nevertheless worth having a glimpse on the analytic continuation of the Breit-frame results.

5.1 Breit Frame

First we want to check, whether analytic continuation from space- to timelike momentum transfers is a reasonable procedure at all. To this aim we compare the form factors of a direct decay calculation with the analytic continuation of scattering form factors for backward-scattering kinematics (which corresponds to the Breit-frame for $\gamma^* M \to M'$). Energetically backward scattering is closest to the decay kinematics for which the invariant mass squared of the decaying system is m_B^2 =const. By fixing the scattering angle, s becomes a unique function of $q^2 = -Q^2$. For a given Q^2 and backward scattering it attains its smallest possible (physical) value. The replacement $Q \to \imath Q$ thus means not only analytic continuation in Mandelstam t, but at the same time also analytic continuation in Mandelstam s. The outcome of the (naive) analytic continuation $Q \to \imath Q$ for the form factor F_1 is compared with the direct decay calculation (see Ref. [GR11]) of B$\to$D and B$\to \pi$ in Figs. 5.1 and 5.2, respectively. At $q^2 = 0$ both results agree, as expected. Approximate agreement is observed up to $q^2 \simeq 8$ GeV^2. At higher q^2 the differences increase and become significant towards the zero-recoil point $q^2 = (m_B - m_D)^2$. We interpret this behavior in such a way that the Breit-frame expressions for the $q^2 < 0$ form factors are not the most appropriate ones to start with when performing the analytic continuation $Q \to \imath\, Q$. Since our form factors for $q^2 < 0$ are s dependent due to violation of cluster separability the analytically continued Breit-frame form factors also pick up this unwanted s-dependence. For the directly calculated decay form factors this would correspond to a dependence on the momentum-transfer squared between the decaying B meson and the neutrino. We cannot exclude a priori that our decay form factors contain such contributions due to wrong cluster properties, but it is neither necessary for the covariant analysis of our decay current to assume such contributions nor is it possible to identify them in a unique way. It therefore seems to be preferable to start from form-factor expressions in a frame in which cluster-separability violating effects are minimized, i.e. the $s \to \infty$ limit (infinite-momentum frame), and apply analytic continuation to these expressions. This has also the advantage that s does not change and thus the continuation procedure might be less delicate.

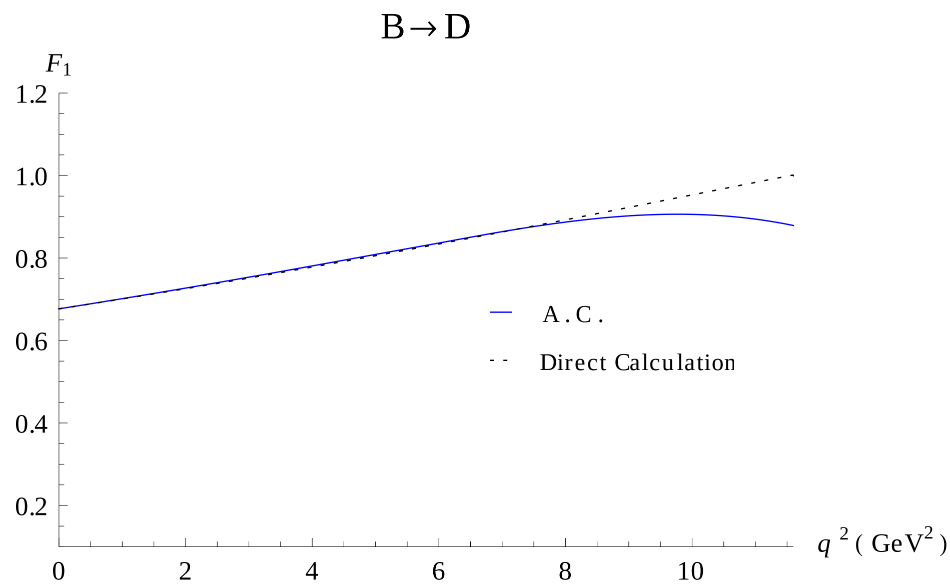

Figure 5.1: This figure shows the analytic continuation of the form factor F_1 calculated in the Breit-frame (solid line) in comparison with the decay result of [GR11] (dashed line) for semileptonic B-D transitions.

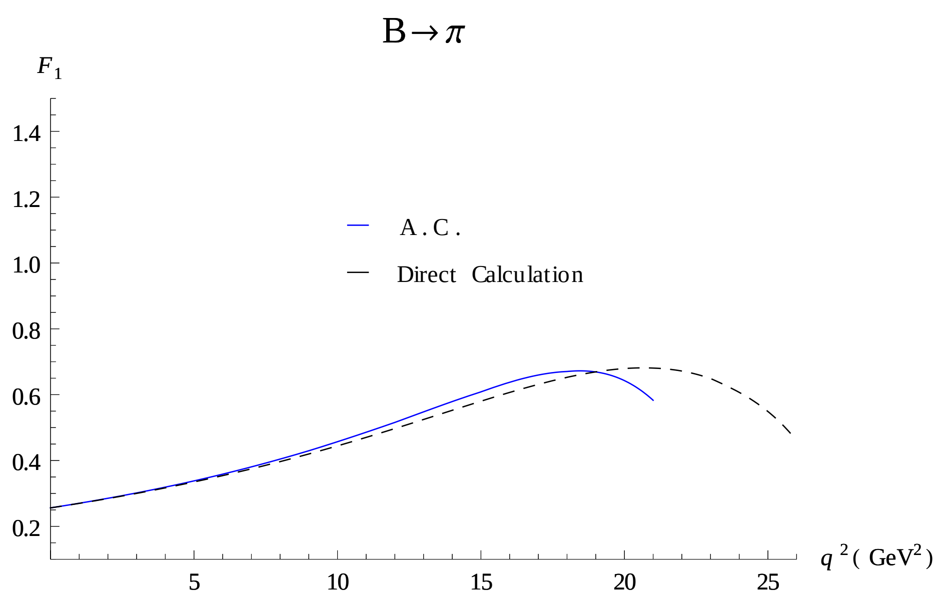

Figure 5.2: Same as fig. 5.1 only for semileptonic B-π transitions.

5.2 Infinite-Momentum Frame

In this section we will present our results for transition form factors for space- as well as timelike momentum transfers, as obtained by analytic continuation of the infinite-momentum-frame results. The comparison with the results obtained in [GR11] will give an estimate for the importance of Z-graphs. To verify the appearance of such quark-pair contributions in our approach, we will analyze the pole structure induced by the mass of the involved resonance. Some effort is also made to point out the quantitative significance of our results by the comparison with lattice results.

We have already argued at the beginning of this chapter that, if one includes all possible graphs to calculate the transition current, the analytic continuation of the scattering form factors leads to the timelike decay form factors. As we said it is also known, that in the $q^+ = 0$ frame in front-form dynamics and in the infinite-momentum frame in instant-form dynamics, Z-graph contributions are suppressed and one obtains the full physical current without considering them. For decay kinematics the $s \to \infty$ limit would correspond to infinitely large momentum transfer between decaying meson and outgoing neutrino, or equivalently, infinitely large invariant mass of outgoing meson and outgoing electron. This is, however, not possible, as long as the decaying meson has finite mass. Therefore one does not have an analogue of the infinite-momentum frame for decay kinematics. But with the usual decay kinematics, starting with the decaying meson at rest, one cannot be sure that Z-graph contributions will not play a role. In [GR11] electroweak form factors of heavy-light mesons for both, space- and timelike momentum transfer, had been computed in a pure valence-quark model using a point form approach for the very first time. In figures 5.3-5.6 we compare these results for various heavy-light transition form factors to our results obtained by means of analytic continuation of the infinite-momentum-frame form factors. We stress that quark-antiquark pair production is known to be suppressed for an infinitely fast moving hadronic system and the difference in the above mentioned figures therefore should give an estimate for the role of Z-graphs. We see that they must obviously be considered for q^2 approaching zero recoil where the results deviate significantly. This high q^2 behavior, especially for the $B \to \pi$ form factor is comparable with predictions in Refs. [CHZ97] and [FaGa14]. In section 5.3, we will motivate how this behavior near zero recoil can be explained if we assume Z-graphs to be implicitly included in our analytic continuation.

Experimental data are hard to obtain near zero recoil, where analytic continuation and direct calculation differ most. Therefore, to proof the significance of our results and to strengthen our argumentation, we compare our infinite-momentum-frame data to form factors calculated on the lattice [lattice01]. This comparison is shown in Tab. 5.1. Despite the fact, that we are using a very simple model to describe the bound-state meson wave functions, our results agree rather well with the lattice values, especially for the $B \to \pi$ transition where we agree almost within one σ.

$B \to \pi$

q^2	Lattice Result [lattice01]	Infinite Momentum Frame
13.6	$F_1 = 0.70(9)^{+.10}_{-.03}$	$F_1 = 0.71$
	$F_0 = 0.46(7)^{+.05}_{-.08}$	$F_0 = 0.42$
15.0	$F_1 = 0.79(10)^{+.10}_{-.04}$	$F_1 = 0.82$
	$F_0 = 0.49(7)^{+.06}_{-.08}$	$F_0 = 0.44$
17.9	$F_1 = 1.05(11)^{+.10}_{-.06}$	$F_1 = 1.15$
	$F_0 = 0.59(6)^{+.04}_{-.10}$	$F_0 = 0.51$
20.7	$F_1 = 1.53(17)^{+.08}_{-.11}$	$F_1 = 1.75$
	$F_0 = 0.71(6)^{+.03}_{-.10}$	$F_0 = 0.59$

$D \to \pi$

q^2	Lattice Result [lattice01]	Infinite Momentum Frame
0.47	$F_1 = 0.67(6^{+.01}_{-.00}$	$F_1 = 0.74$
	$F_0 = 0.62(6)^{+.02}_{-.00}$	$F_0 = 0.67$
0.97	$F_1 = 0.81(7)^{+.02}_{-.00}$	$F_1 = 0.88$
	$F_0 = 0.70(6)^{+.01}_{-.00}$	$F_0 = 0.71$
1.48	$F_1 = 1.03(9)^{+.01}_{-.00}$	$F_1 = 1.07$
	$F_0 = 0.80(6)^{+.01}_{-.00}$	$F_0 = 0.75$

$D \to K$

q^2	Lattice Result [lattice01]	Infinite Momentum Frame
0.19	$F_1 = 0.70(5)(0)$	$F_1 = 0.79$
	$F_0 = 0.68(4)(0)$	$F_0 = 0.76$
0.69	$F_1 = 0.84(5)(0)$	$F_1 = 0.91$
	$F_0 = 0.76(4)(0)$	$F_0 = 0.79$
1.7	$F_1 = 1.29(7)(0)$	$F_1 = 1.27$
	$F_0 = 0.96(4)(0)$	$F_0 = 0.84$

Table 5.1: Form factors F_1 and F_0 obtained by analytic continuation of the infinite-momentum-frame results in comparison with lattice data [lattice01].

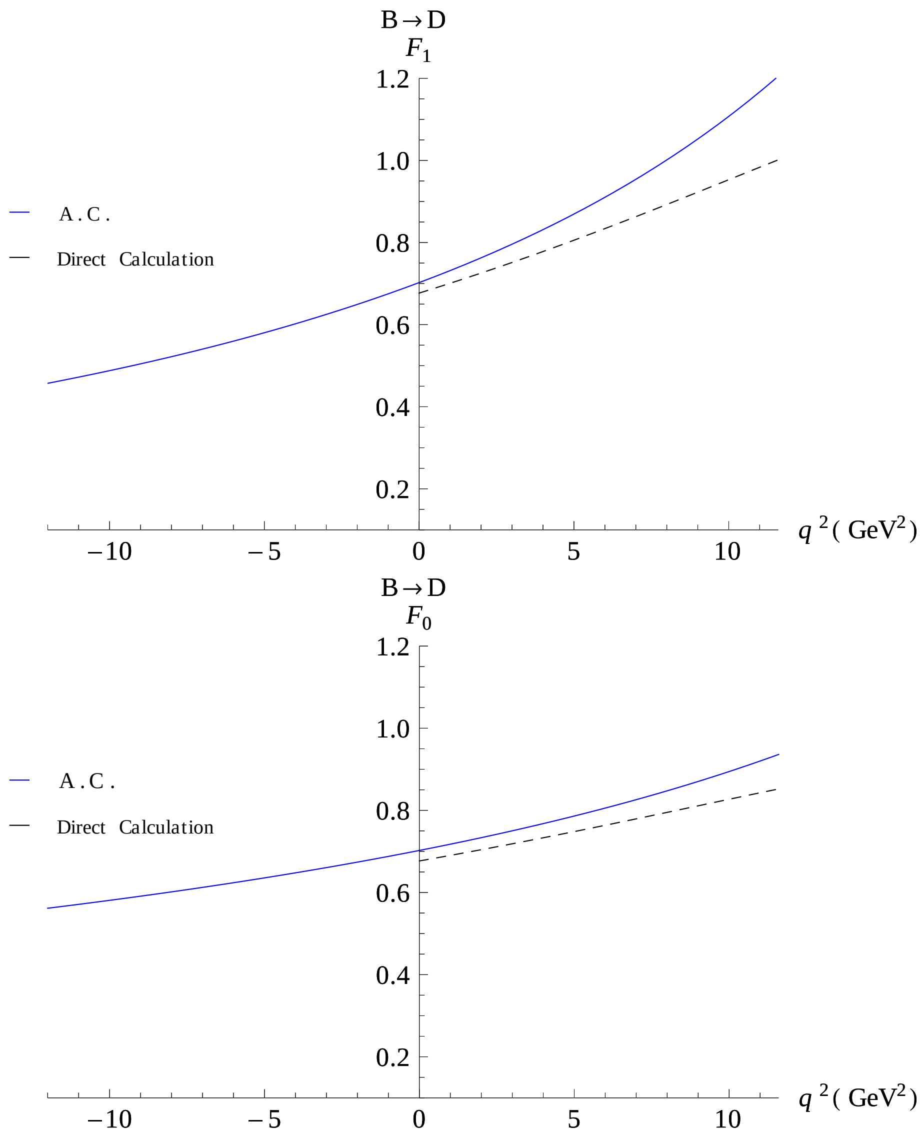

Figure 5.3: Form factors F_1 and F_0 obtained by analytic continuation of the infinite-momentum-frame results (solid line) compared to the direct decay results of [GR11] (black dashed line) for B-D transitions.

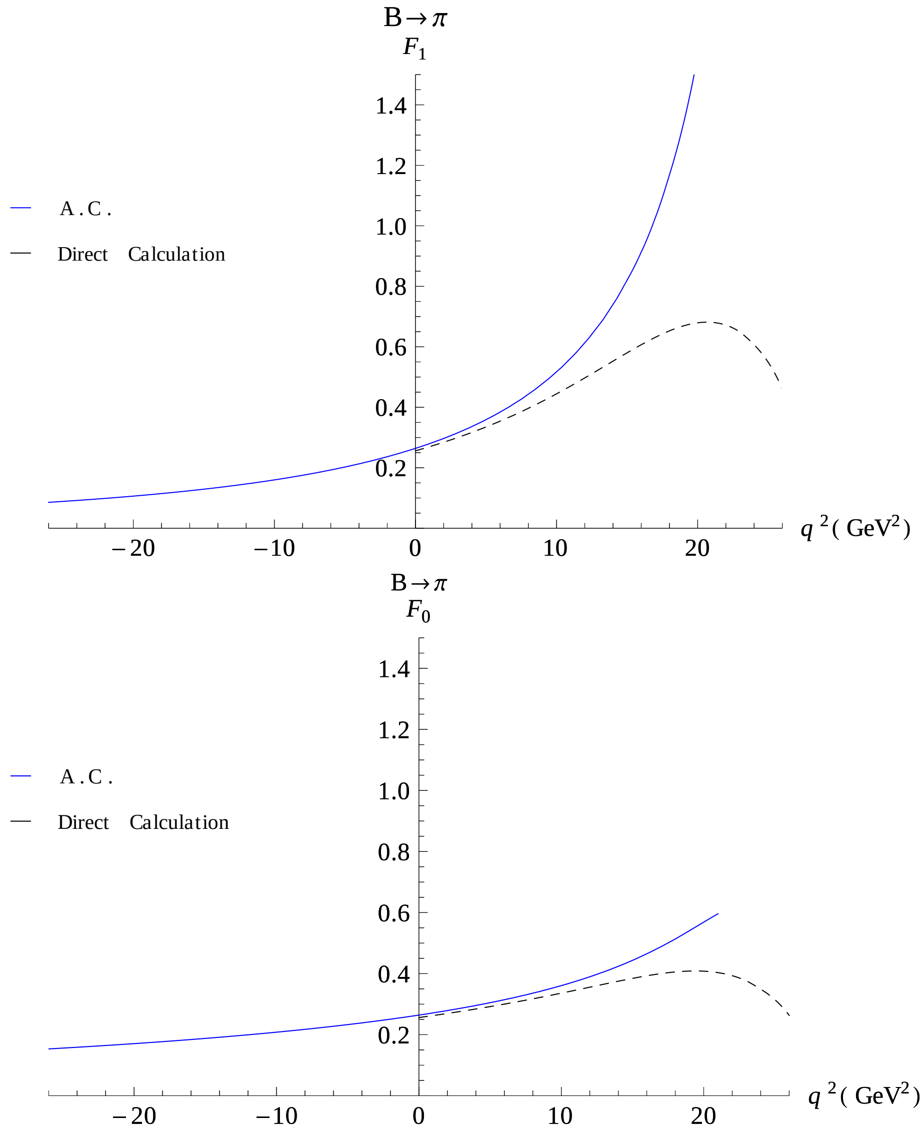

Figure 5.4: Form factors F_1 and F_0 obtained by analytic continuation of the infinite-momentum-frame results (solid line) compared to the direct decay results of [GR11] (black dashed line) for B-π transitions.

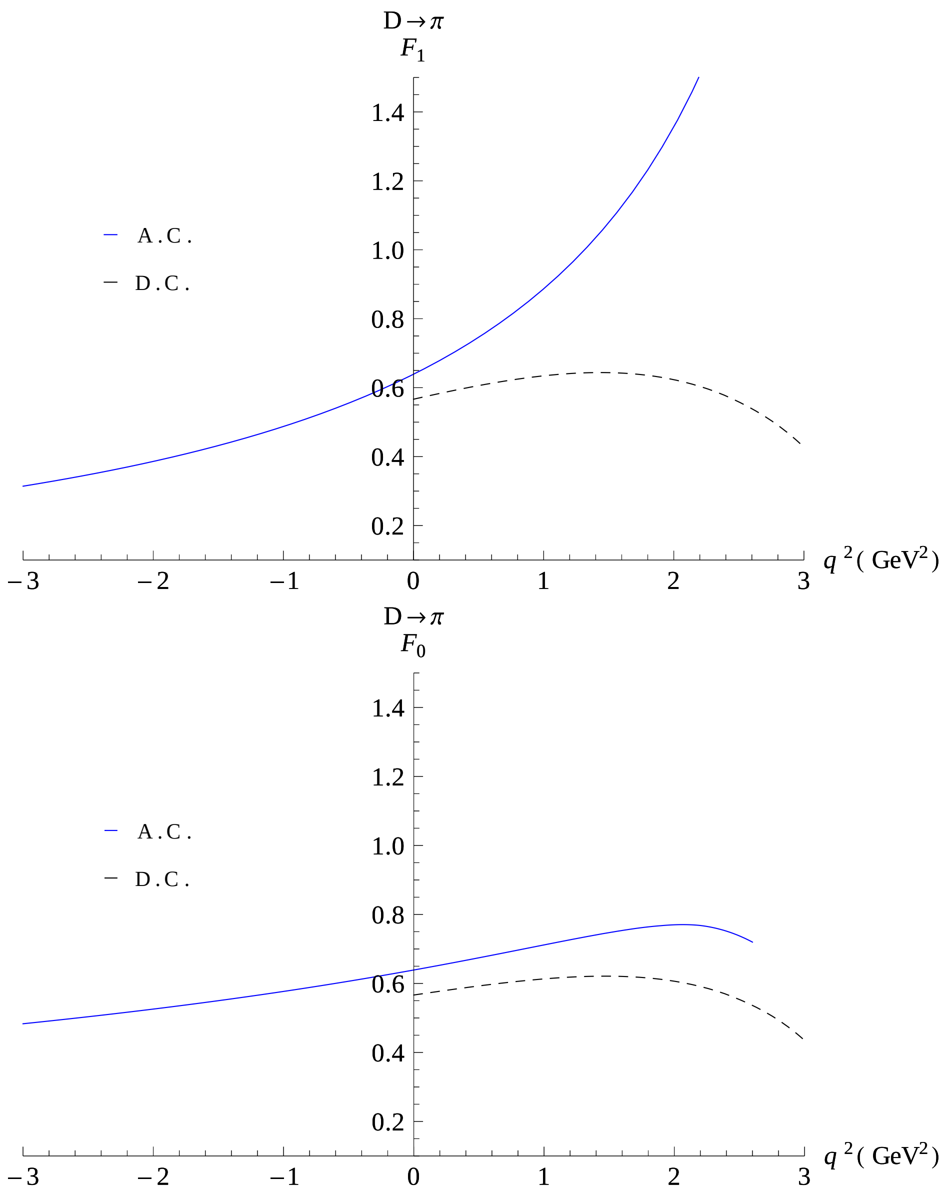

Figure 5.5: Form factors F_1 and F_0 obtained by analytic continuation of the infinite-momentum-frame results (solid line) compared to the direct decay results of [GR11] (black dashed line) for D-π transitions.

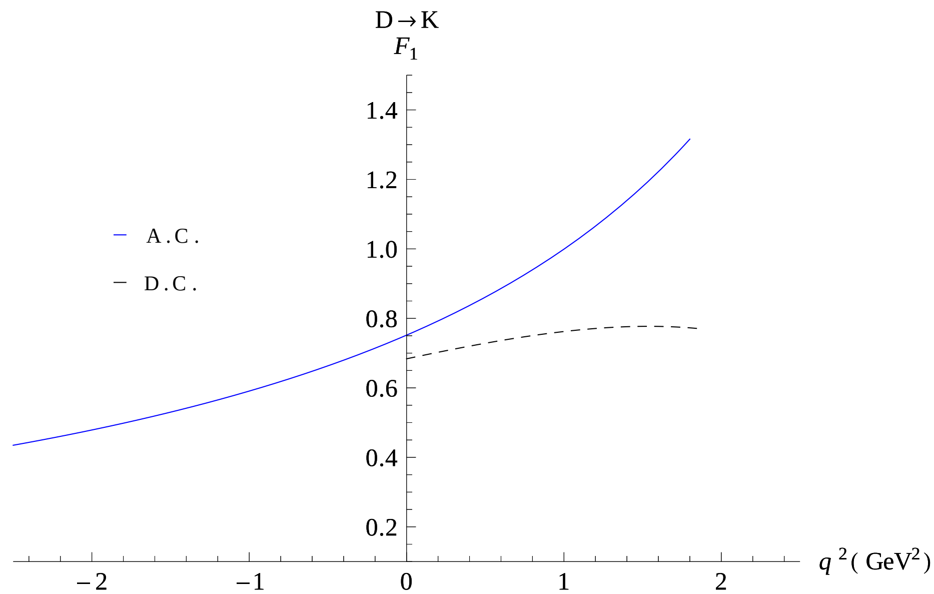

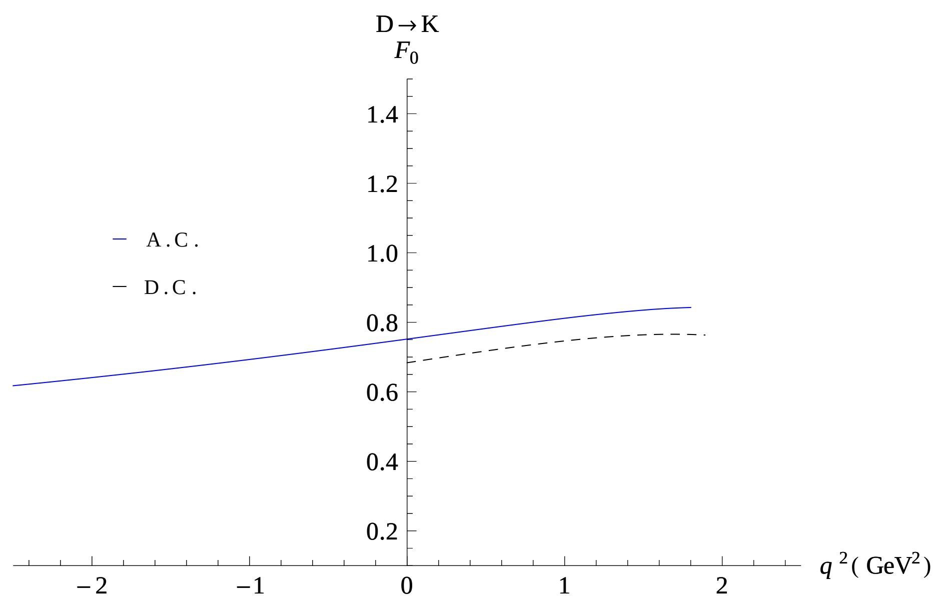

Figure 5.6: Form factors F_1 and F_0 obtained by analytic continuation of the infinite-momentum-frame results (solid line) compared to the direct decay results of [GR11] (black dashed line) for D-K transitions.

5.3 Z-Graph and Meson Pole

The foregoing results suggest that Z-graph contributions should be included explicitly in a direct decay calculation. Since we use instantaneous confinement throughout, the non-valence degrees-of-freedom arising from quark-antiquark vacuum fluctuations have to recombine with the existing $Q\bar{q}$ pair to color singlet hadrons. This is most simply described by the occurrence of an intermediate vector meson M^* (in addition to the final meson M'). This mechanism, seen in a constituent-quark-model point of few, is depicted in Fig. 5.7. In the literature such contributions are included in different ways.

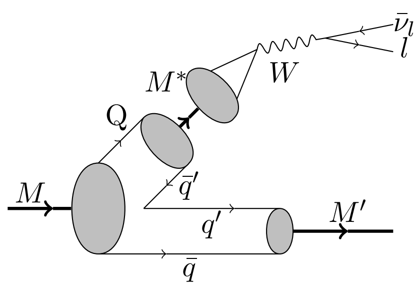

Figure 5.7: Z-graph contribution to the semileptonic $M \to M'$ decay within a constituent quark picture. M^* could, for example, be the $B_c^{+\,*}$ resonance appearing in a $B^+ \to D^0$ decay.

In [CHZ97], for example, the initial state of the decaying meson is described as a composite state of a bare meson and a two-particle state consisting of the M^* and the outgoing meson M'. Similar a decay constant and an effective Hamiltonian density for the M^*MM' vertex, with a soft hadronic vertex form factor, had been used in [IW90]. In [CHZ97] the authors analyzed the valence and Z-graph contributions separately for the semileptonic $B \to \pi$ decay. They found that in the low q^2 regime the valence contribution to the form factor F_1 has a pole structure

$$F_1^{\text{pole}}(q^2) = \frac{F_1(0)}{(1 - \frac{q^2}{M_{\text{pole}}^2})^\alpha} \tag{5.1}$$

with $\alpha = 1.6$ and $M_{\text{pole}} = 5.32\text{GeV}$, whereas near zero recoil, F_1 decreases as q^2 increases. This behavior resembles the direct decay results of [GR11] in Fig. 5.4. The combined valence and Z-graph results of [CHZ97] follow Eq.(5.1) in the whole kinematic region, if parameters $\alpha = 2$ and $M_{\text{pole}} =$

6.0GeV are used. Putting both together a strong increase at zero recoil is observed which cannot be explained by the valence contribution alone. Fig. 5.3 shows our attempt to parametrize our results for F_1 in case of $B \to D$ and $D \to K$ transitions, as obtained by analytic continuation, by means of Eq. 5.1. Thereby the mass of the lightest possible vector meson M^* is taken for M_{pole}. We find that our results (coming from analytic continuation) follow Eq. (5.1) rather well in the whole kinematic range, with $\alpha_{B\to D} = 1.55$ and $\alpha_{D\to K} = 1.09$. The strong increase of the form factor near zero recoil, indicating a nearby pole, is an evidence for a vector-meson-dominance like mechanism in which the $M \to M'$ transition happens through emission of a vector meson M^* which subsequently decays into the lepton pair via W exchange. On the quark level this kind of process can only happen via a non-valence $Q\bar{q}q\bar{q}$ component of the decaying meson M which then leads to the Z-graphs we are interested in. Taking such contributions explicitly into account would require some additional modeling of the non-valence component. One possibility, e.g., would be to create the non-valence component from the valence component by means of a $^3P_0$-vertex which creates the additional $q\bar{q}$-pair out of the vacuum [SEF12]. This is the kind of mechanism depicted in Fig.5.7. In view of these considerations it is somehow surprising that our analytic continuation procedure provides a pole-like behavior near zero recoil, although non-valence contributions have not been taken into account explicitly. However, due to the analyticity of the scattering amplitude it is clear that, if we include all nonvanishing contributions for a specific kinematics, we can obtain a result in another kinematical region, also containing all nonvanishing contributions. This confirms the validity of the repeatedly stated argument, that one does not have to include Z-graphs explicitly in the infinite-momentum-frame to obtain the full physical current in the point form of relativistic dynamics and that most of the physics is already contained in the valence contribution. From this point of view the different frame dependencies of space-like form factors, which we discussed in section 4.3, become plausible. The position of the pole is determined by the mass squared of the intermediate resonance. In other words, the smaller the mass of the resonance, the smaller the distance of the maximum recoil point to the pole, the higher the effect on the form factors in the space-like momentum transfer region. The different masses of incoming, outgoing and intermediate states are shown in Tabs. 5.2. For all $B \to X$ transitions the resonance lies much further apart from maximum recoil than for all $D \to X$ transitions. This explains why the differences between infinite-momentum-frame results and Breit-frame results are larger for $D \to X$ transitions than for $B \to X$ transitions. $D \to X$ must consequently show

Table 5.2: Meson masses and resonances

Transition	Initial Meson	Final Meson	Resonance
$B^- \to D^0$	$M_{B^-} = 5.2795$ GeV	$M_{D^0} = 1.869$ GeV	$M_{B_c^*} > M_{B_c} = 6.274$ GeV
$\bar{B}^0 \to \pi^+$	$M_{\bar{B}^0} = 5.2795$ GeV	$M_{\pi^+} = 1.869$ GeV	$M_{B^*} = 5.325$ GeV
$\bar{B}^0_S \to K^+$	$M_{\bar{B}^0_S} = 5.3667$ GeV	$M_{K^+} = 0.4937$ GeV	$M_{B^*} = 5.325$ GeV
$\bar{D}^0 \to K^+$	$M_{\bar{D}^0} = 1.864$ GeV	$M_{K^+} = 0.4937$ GeV	$M_{D_s^{*-}} = 2.112$ GeV
$D^- \to \pi^0$	$M_{D^-} = 1.869$ GeV	$M_{\pi^0} = 0.135$ GeV	$M_{D^{*-}} = 2.010$ GeV

a greater frame dependence than $B \to X$ transitions.

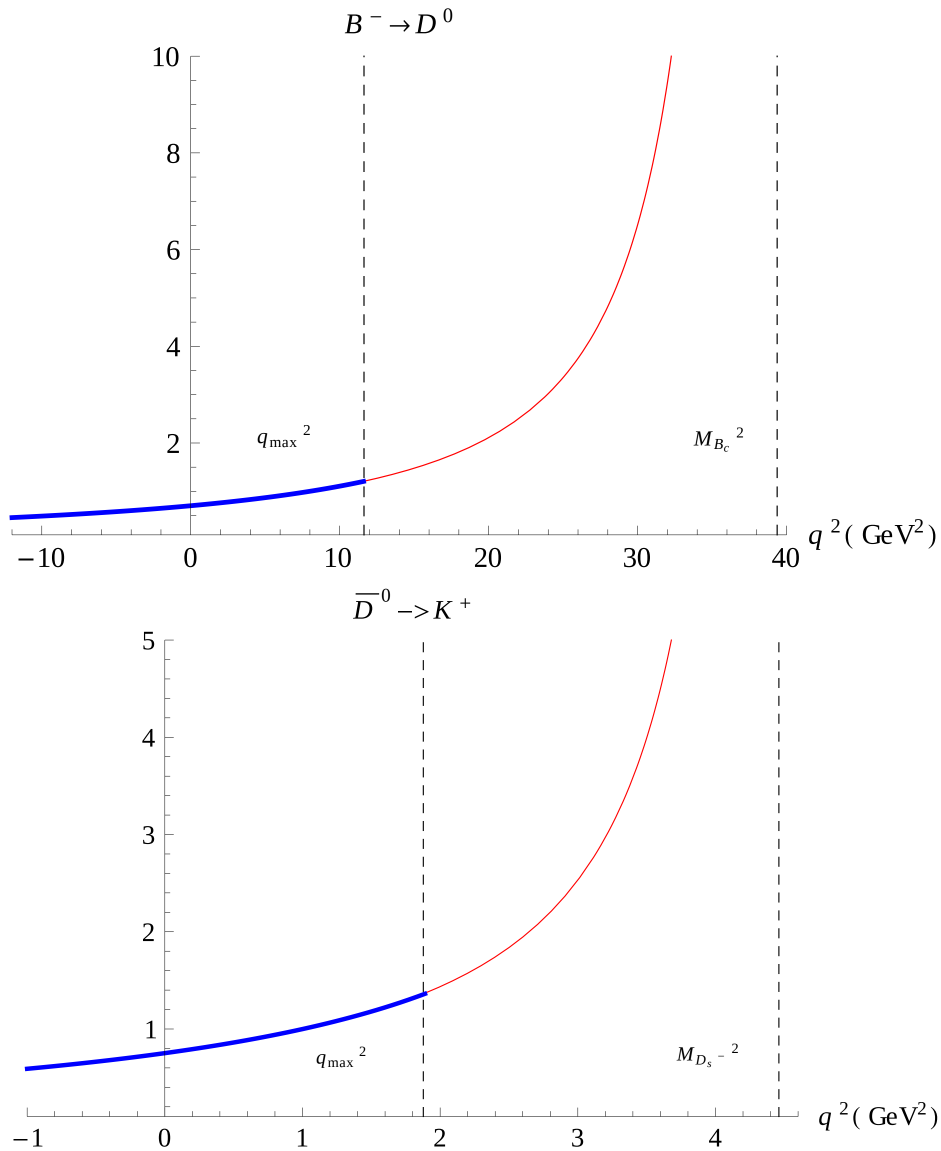

Figure 5.8: $B^- \to D^0$ (top) and $\bar{D}^0 \to K^+$ (bottom) transition form factors F_1 for space- and timelike momentum transfer (thick line) and pole fit $F_1^{\text{pole}}(q^2)$ (thin line) with $\alpha_{B\to D} = 1.55$ and $M_{\text{pole}} = M_{B_c} = 6.274$ GeV (top) and $\alpha_{D\to K} = 1.09$ and $M_{D_S^-} = 2.112$ GeV (bottom). The position of zero recoil and M^2_{pole} are indicated by the dashed vertical lines.

Chapter 6

Heavy-Quark Symmetry

In this chapter we will focus on heavy-quark symmetry and confront our results with available experimental data. A consequence of heavy-quark symmetry is, that the heavy-light meson wave function becomes independent of flavor and spin of the heavy quark as the heavy-quark mass goes to infinity. In [GRS12] the preservation of heavy-quark symmetry had been proved for the point-form approach to form factors applied also in the present work. It was demonstrated that the electromagnetic scattering and semileptonic decay form factors of pseudoscalar mesons approach a universal form factor, the Isgur-Wise function, if one performs the heavy-quark limit. This limit has to be taken such, that the velocity product

$$v_{\alpha'} \cdot v_{\alpha} = \frac{k_{\alpha'} \cdot k_{\alpha}}{m_{\alpha} m_{\alpha'}} \tag{6.1}$$

stays constant, while $m_Q = m_\alpha$ and $\frac{m_q}{m_Q} = 0$ for $m_Q \to \infty$. Since we don't want to deal with subtleties of the heavy-quark limit, we refer to [IW89], [IW90] and [GRS12] for a detailed discussion. What we are rather interested in, is the effect of Z-graphs on heavy-quark symmetry (breaking). It is plausible that for an analogous reason as in the case of infinite momentum, Z-graphs involving heavy quarks should be suppressed in the heavy-quark limit. The probability for the vacuum to fluctuate into an infinitely heavy quark-antiquark pair should vanish. The transition we want to investigate is the $B^- \to D^0$ transition. Assuming that Z-graph contributions are accounted for by our analytic continuation procedure, the production of a heavy $c\bar{c}$ quark-antiquark pair leads to the contribution shown in Fig. 5.7. In Fig. 6.1 we see that suppression of $c\bar{c}$ production out of the vacuum is indeed well described by our model. In the upper panel the physical meson

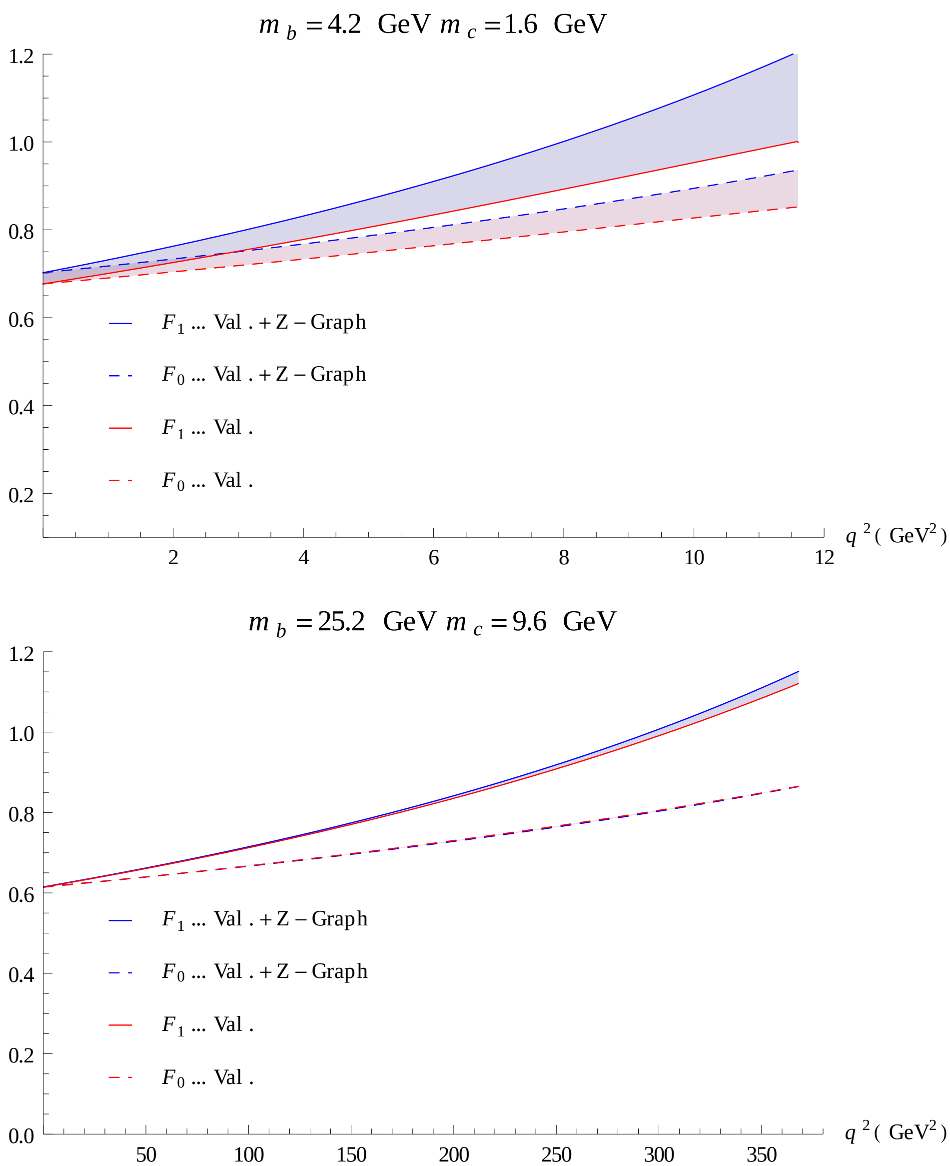

Figure 6.1: Form factors F_1 and F_0 with and without Z-graphs for physical meson and constituent masses (top) and considerable larger heavy-quark masses (bottom).

and constituent masses are used whereas in the lower panel the constituent masses are multiplied by a factor 6 and the meson masses are set equal to the heavy-quark masses. As expected the differences attributed to Z-graphs (shaded areas) vanish in both, F_1 and F_0 as the masses of the heavy quarks become considerably larger. So we can conclude that the extension of the Bakamjian-Thomas point-form approach with respect to non-valence degrees-of-freedom does not spoil heavy-quark-symmetry properties.

Z-graphs do not spoil heavy-quark symmetry in the heavy-quark limit, but they might well influence heavy-quark-symmetry breaking for physical quark masses. To demonstrate the amount of symmetry breaking we present the form factors of Fig 6.1 as functions of the product $v_{\alpha'} \cdot v_\alpha$, which is a widely used representation for the discussion of heavy-quark symmetry. In order to allow for a comparison with the Isgur-Wise function, the form factors are multiplied with appropriate kinematic factors

$$\begin{aligned} F_1 &\to R F_1, \\ F_0 &\to \frac{R}{1 - \frac{q^2}{(M_B+M_D)^2}} F_0, \\ R &= \frac{2\sqrt{M_B M_D}}{M_B + M_D}. \end{aligned} \tag{6.2}$$

What we then find is, that in contrast to [GRS12] (dashed lines), the form factors including Z-graphs (dotted lines) fall almost together already for physical meson and constituent masses (cf. Fig. 6.2). This is what one would expect from heavy-quark symmetry. The deviation from the Isgur-Wise function is almost independent from $v_\alpha \cdot v_{\alpha'}$ which is definitely not the case for the curves which correspond to the valence part only. It looks as if the Isgur-Wise function for finite b- and c-quark masses was just a slightly rescaled version of the one obtained in the heavy-quark limit. On the other hand, the average deviation from the Isgur-Wise function in the $v \cdot v'$ range corresponding to $q^2 \in [0, (M_B - M_D)^2]$:

$$\begin{aligned} \sigma_{F_1}^{\text{val+Z-graph}} &= 10.6\% \quad & \sigma_{F_0}^{\text{val+Z-graph}} &= 10.7\% \\ \sigma_{F_1}^{\text{val}} &= 5.3\%, \quad & \sigma_{F_0}^{\text{val}} &= 5\% \end{aligned}$$

is larger for the full calculation than for the decay calculation involving valence contributions only. With upscaled heavy-quark masses the influence of Z-graphs is seen to shrink and heavy-quark symmetry is gradually restored with all the curves tending to the Isgur-Wise function in the heavy-quark limit.

Finally we would like to give a comparison with experimental data. What one can measure experimentally is the slope of F_1 as function of $v \cdot v'$ at zero recoil. To be more precise, the quantity which we compare is defined as

$$\rho_D^2 := -\frac{F_1'(vv'=1)}{F_1(vv'=1)}. \tag{6.3}$$

The experimental value given by the heavy-flavor averaging group [HFAG10] is $\rho_D^2 = 1.18 \pm 0.06$. In [GRS12] the direct decay calculation involving only valence degrees-of-freedom gave a value of $\rho_D^2 = 0.59$. We confirm this finding. On the other hand, our analytic continuation procedure which implicitly seems to account for Z-graph contributions (in the time-like regime) provides a value of $\rho_D^2 = 1.07$, much closer to experiment than the direct decay calculation. This hints at the necessity to include Z-graph contributions in the direct decay calculation.

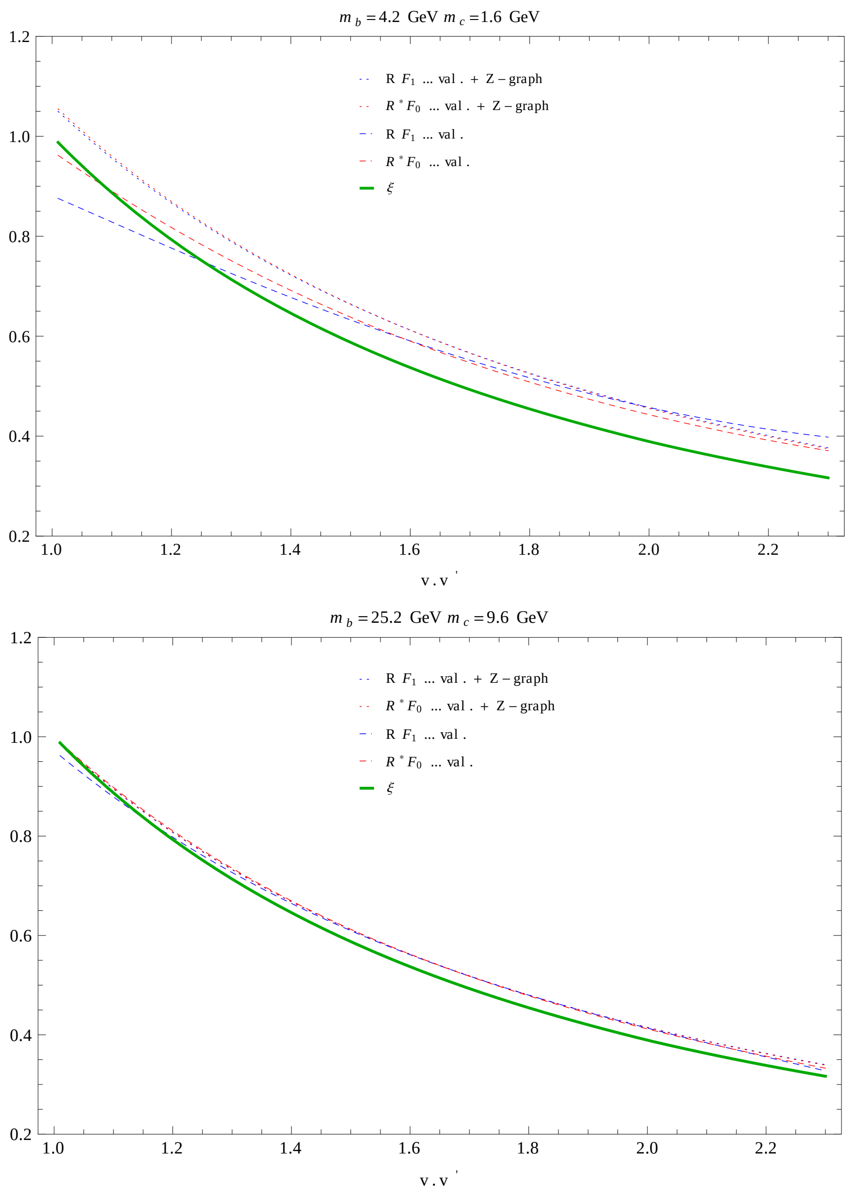

Figure 6.2: Weak $B \to D$ transition form factors as functions of $v_{\alpha'} \cdot v_\alpha$ (multiplied with appropriate kinematical factors) in comparison with the Isgur-Wise function resulting from the heavy-quark limit.

Chapter 7

Summary and Outlook

The present diploma thesis has extended foregoing work on the theoretical determination of the electroweak structure of hadrons within relativistic point-form quantum mechanics using constituent-quark models. Our aim was to calculate weak transition form factors of pseudoscalar heavy-light mesons for space- as well as timelike momentum transfers. Such form factors could, in principle, be measured in neutrino-meson scattering and in semileptonic weak meson decays, respectively. Our theoretical framework was the point form of relativistic quantum mechanics and the Bakamjian-Thomas construction for implementing the weak and the confining interactions in a Poincaré-invariant way. Starting with an appropriate multichannel mass operator we were able to derive the invariant 1-W-exchange scattering amplitude. From this amplitude we could separate the weak meson transition current and identify the weak transition form factors by means of a covariant decomposition of this current.

Starting with neutrino-meson scattering, we have first derived weak transition form factors for heavy-light to heavy-light and light-light meson transitions in the spacelike momentum-transfer region. As in the foregoing work on electromagnetic hadron form factors we found that these transition form factors are not only functions of Q^2, the squared momentum transfer between incoming and outgoing meson, but depend also (slightly) on Mandelstam s, the squared invariant mass of the neutrino-meson system. This s dependence of the weak transition form factors is the consequence of wrong cluster properties inherent in the Bakamjian-Thomas construction. It does not violate relativistic invariance of our neutrino-meson scattering amplitude, but rather indicates that the WMM'-vertex is affected by the presence of the electron. This s dependence may also be interpreted as a frame-dependence of the $W^*M \to M'$ subprocess. We have estimated this frame dependence by choosing two extreme cases, namely $s \to \infty$ and minimal s to reach a particular Q^2. For the $W^*M \to M'$ subprocess the first case corresponds to the infinite-momentum frame, the second case to the Breit frame. For the $B \to D$, π transition form factors these differences turned out to be marginal, whereas they can amount to about 10% for $D \to K$, π transitions. From the foregoing investigations of electromagnetic form factors for spacelike momentum transfers it is known that the results of our point-form calculations in the infinite-momentum frame are equivalent with corresponding front-form calculations in the $q^+ = 0$ frame. We suppose that this equivalence does also hold for the weak transition form factors we are interested in, although we have not checked it explicitly. The $q^+ = 0$ frame in front form has the big advantage that Z-graph contributions to the form factors, which are caused by non-valence components of the hadrons, vanish due to kinematical reasons, whereas such contributions can become sizable in other frames, like the Breit frame. Analogously, in point-form Z-graphs are also suppressed in the infinite-momentum frame due to kinematical reasons, whereas it cannot be precluded that they play a role in any other frame. It is even suspected that they could partly reconcile the observed frame dependence of the form factors. In this sense, the infinite-momentum frame seems to be preferable to any other frame if one sticks to a pure valence-quark description of form factors.

Our next goal was to extend our form factor calculations to timelike momentum transfers. Following our strategy this could be done by applying our relativistic multichannel framework to semileptonic weak decays, calculate decay amplitudes, separate the weak hadronic transition current and identify the weak transition form factors. In foregoing work the weak transition form factors have indeed been derived along these line. Since the invariant mass of the initial state, i.e. the decaying meson, is fixed, the form factors were found to depend only on the squared four-momentum transfer between decaying and outgoing meson, as it should be. But this also means that there is no way for the decay calculation to choose a particular frame for the $M \to W^*M'$ subprocess such that the influence of Z-graph contributions could be minimized. A similar situation occurs in front form, where $q^+ = 0$ is simply forbidden by the decay kinematics. From front-form calculations with a simple scalar model – for which one could calculate the complete covariant triangle diagram – one furthermore knows that Z-graphs are by no means negligible for decay kinematics. The full form factor for the scalar model could, however, be recovered by analytic continuation of the pure valence contribution obtained for space-like momentum transfers in a $q^+ = 0$ frame. This was also our motivation to take the form factors for spacelike momentum transfers, obtained in the infinite-momentum frame, and continue them analytically to timelike momentum transfers. The results from this analytic continuation procedure turned out to be comparable with lattice results and also the slope of $F_1^{B\to D}$ at the zero recoil point, i.e. maximum timelike momentum transfer, was found to be compatible with experiment. Unfortunately there are no other experiments to compare with. Already for $B \to D$ decays the form factors coming from analytic continuation and from the direct decay calculation were found to differ significantly. For $B \to \pi$ and $D \to K$, π decays these differences became even larger. We interpret these differences as a sign for the missing Z-graph contributions in the direct decay calculation. The size of these differences then gives us a rough estimate for the absolute magnitude of Z-graph contributions. We have also checked that these differences vanish in the heavy-quark limit, which means that Z-graphs do not play a role in this limit. This is easily understood since an infinitely heavy quark-antiquark pair cannot be created out of the vacuum. Contrary to previous finding we saw also that the frame dependence of the $B \to D$-transition form factors vanishes in the heavy-quark limit and we could verify that all the properties connected with heavy-quark symmetry are satisfied.

A more quantitative analysis of Z-graph contributions would require some additional modeling. For $B \to D$ decays, e.g., Z-graphs would arise from a non-valence $b\bar{u}c\bar{c}$ component in the B. With instantaneous confinement this could equivalently be described on the hadronic level as a DB_c^* component in the B. Z-graph contributions to semileptonic weak decays can then be simply understood via a vector-meson-dominance like mechanism in which the B decays (virtually) into D and B_c^*, the B_c^* then fluctuates into a W, which finally decays into the lepton pair. This kind of mechanism gives rise to an enhancement of the form factors near the zero-recoil point via the presence of the B_c^* pole at timelike momentum transfers much larger than accessible by physical decay processes. For B decaying into light mesons and for D decays this pole comes closer to the zero-recoil point and the enhancement is expected to become stronger. Exactly this kind of behavior is mimicked by our form factor predictions coming from the analytic-continuation procedure. Surprisingly we found that these predictions could even be fitted over a wide space- and timelike momentum-transfer range with a function close to a monopole and the physical $B^*_{(c)}$ and $D^*_{(s)}$ masses determining the pole position.

Having understood that Z-graphs on the quark level give rise to a vector-meson-dominance like mechanism, as long as one works within constituent-quark models with instantaneous confinement, the explicit calculation of Z-graphs is considerably simplified. The whole calculation can essentially be done on the hadronic level. The only input to be determined on the quark level are the VMM'-vertex (V being the intermediate vector meson) and the VW-coupling. For both quantities one has to know the M, M' and V wave functions. For the vertex one has to specify, in addition, how the non-valence quark-antiquark pair, necessary for the $M \to M'V$ transition, is created. This could, e.g., be accomplished by means of the widely used $^3P_0$ model. Calculations along these lines will be the subject of future work and will hopefully give us a more quantitative understanding of the role of Z-graphs in semileptonic weak decays and also in neutrino-meson scattering in frames different from the infinite-momentum frame.

Acknowledgements

First of all I would like to thank my supervisor Ao. Univ.-Prof. Mag. Dr. Wolfgang Schweiger for his constantly advise and for his time in which we extensively discussed my questions and concerns. His deep understanding of physics accompanied by his kindness and modesty inspire me.
I am also glad to thank Dr. María Gómez-Rocha who always happily explained her work to me. I can not overestimate the value of our discussions.

At some point in life as well as in science understanding can only follow acceptance, for nature in it's inmost will not bend to our way of thinking. A lesson that took me some time to learn, and I would like to thank my parents for their never-ending support and their confidence in me during doing so. It is not something I take for granted. There are so many people who I am glad to call friends. Thank you all for being part of my life. My final thanks belong to Anja. You have enlightened my way, never stop doing so.

Bibliography

[BCJ03] B.L.G Bakker, H.-M. Choi and C.-R. Ji, “Transition form-factors between pseudoscalar and vector mesons in light front dynamics.” Phys. Rev. D 67, 113007 (2003).

[Biernat11] E.P. Biernat, “Electromagnetic properties of few-body systems within a point-form approach.” PhD. thesis, University of Graz (2011) arXiv:1110.3180 [nucl-th].

[BSFK09] E.P. Biernat, W. Schweiger, K. Fuchsberger, W. H. Klink, “Electromagnetic meson form factor from a relativistic coupled-channel approach.” Phys. Rev. C 79, 055203 (2009).

[BT53] B. Bakamjian and L.H. Thomas, “Relativistic particle dynamics 2.” Phys. Rev. 92, 1300 (1953).

[CCH97] H.-Y. Cheng, C.-Y. Cheung, and C.-W. Hwang, “Mesonic form-factors and the Isgur-Wise function on the light front.” Phys. Rev. D 55, 1559 (1997).

[CHZ97] C.Y. Cheung, C.W. Hwang and W.M. Zhang, “$B \to \pi l \nu$ Form Factors Calculated on the Light-Front.” Z. Phys. C 75, 657 (1997).

[Dir49] P. A. M. Dirac, “Forms of relativistic dynamics.” Rev. Mod. Phys. 21, 392 (1949).

[FaGa14] R.N. Faustov and V.O. Galkin, “Rare $B \to \pi l l^-$ and $B \to \rho l l^-$ decays in the relativistic quark model.” arXiv:1403.4466 [hep-ph] (2014).

[Fuc07] K. Fuchsberger, “Electromagnetic meson form factors within a relativistic coupled-channel approach.” Diploma thesis, University of Graz (2007).

[GR99] F.Gross, "Relativistic Quantum Mechanics and Field Theory." Wiley-Interscience Publication, New York, Chichester, Weinheim, Brisbane, Singapore, Toronto (1999).

[GR11] M. Gomez-Rocha, "Electroweak hadron structure within a relativistic point-form approach." PhD. thesis, University of Graz (2012), arXiv:1306.1248 [hep-ph].

[GRS12] M. Gomez-Rocha and W. Schweiger, "Electroweak form factors of heavy-light mesons-a relativistic point-form approach." Phys. Rev. D 86, 53010 (2012).

[HFAG10] Heavy Flavor Averaging Group Collaboration, D. Asner et al., "Averages of b-hadron, c-hadron, and τ-lepton properties." (2010) arXiv:[hep-ex]10101589.

[IW89] N. Isgur and M.B. Wise,"Weak decays of heavy mesons in the static quark approximation." Phys.Lett. B 232, 113 (1989).

[IW90] N. Isgur and M.B. Wise, " Influence of the B^* resonance on $\bar{B} \to \pi e \bar{\nu}_e$." Phys.Rev. D 41, 151 (1990).

[JISu13] C.-R. Ji and A.T. Suzuki, "Interpolating scattering amplitudes between the instant form and the front form of relativistic dynamics ." Phys.Rev. D 87, 065015 (2013).

[Kli03a] W. H. Klink, "Constructing point form mass operators from interaction Lagrangians." Nucl.Phys. A 716, 123 (2003)

[Kli98] W. H. Klink, "Relativistic simultaneously coupled multi particle states." . Phys.Rev. C 58, 3617 (1998).

[Kra01] A.Krassnigg, "A relativistic point-form approach to quark-antiquark systems. " PhD thesis, University of Graz (2001).

[KP91] B. D. Keister and W. N. Polyzou, "Relativistic Hamiltonian dynamics in nuclear and particle physics." Adv. Nucl. Phys. 20, 225 (1991).

[KSK03] A. Krassnigg, W. Schweiger and W. Klink, "Vector mesons in a relativistic point-form approach." Phys. Rev. C 67, 064003 (2003).

[lattice01] A. Abada, D. Becirevic, PH. Boucaud, J.P. Leroy, V. Lubicz, F. Mescia, "Heavy $\to$ Light semileptonic decays of pseudoscalar mesons from lattice QCD." Nucl. Phys. B 619, 565 (2001).

[MeSi02] D. Melikhov and S. Simula, "Electromagnetic form factors in the light-front formalism and the Feynman triangle diagram: spin-0 and spin-1 two-fermion systems." Phys. Rev. D 65, 0940463 (2002).

[PDG12] J. Beringer et al. [Particle Data Group], "Review of particle physics." Phys. Rev. D 86, 10001 (2012).

[Pol09] W. N. Polyzou. "Poincaré invariant quantum theory, J.Lab lectures." (2009) arXiv:09081441[nucl-th].

[SEF12] J. Segovia, D.R. Entem, F. Fernández, "Scaling of the $3P^0$ strength in heavy meson strong decays." Phys. Lett. B 715, 322 (2012).

[Si02] S. Simula, " Comparison among Hamiltonian light-front formalisms at $q^+ = 0$ and $q^+ \neq 0$: Space like elastic form factors of pseudoscalar and vector mesons." Phys. Rev. C 66, 035201 (2002).

[SW64] R.F.Streater and A.S Wightman, " PCT, Spin and statistics, and all that." W.A.Benjamin Inc, New York, Amsterdam (1964).

[Tha92] B.Thaller, "The Dirac Equation." Springer, Berlin, Heidelberg (1992).

[Tung03] W.K.Tung, "Group Theory in Physics." World Scientific Publishing, Singapore (2003).

[WSB85] M. Wirbel, B. Stech and M. Bauer, "Exclusive Semileptonic Decays of Heavy Mesons," Z. Phys. C 29, 637 (1985).